FACULDADE DE ENGENHARIA DA UNIVERSIDADE DO PORTO

Incremental Redundancy ARQ Communications Schemes applied to High-Efficiency IoT Systems

Sérgio Miguel Marques Ribeiro da Silva

Mestrado em Engenharia Eletrotécnica e de Computadores

Supervisor: Nuno T. Almeida

November 9, 2023

Abstract

The rapid proliferation of Internet of Things (IoT) systems, encompassing a wide range of devices and sensors with limited battery life, has highlighted the critical need for energy-efficient solutions to extend the operational lifespan of these battery-powered devices.

One effective strategy for reducing energy consumption is to minimize the retransmission of data packets in the event of communication errors. Among the array of potential solutions, Incremental Redundancy Hybrid Automatic Repeat reQuest (IR-HARQ) communication schemes have emerged as particularly compelling options.

This work aims to address the challenge by developing a simulator capable of executing, analysing, and validating various tests involving different (H)ARQ schemes. The primary objective is to compare their performance across multiple metrics, enabling a comprehensive evaluation of their capabilities.

The proposed simulator will boast a high level of configurability, offering numerous adjustable parameters across different aspects to accommodate the simulation of a wide array of scenarios. This adaptability will make it possible to recreate various real-world conditions and explore the behaviours of different (H)ARQ strategies under diverse circumstances.

The results indicate that IR-HARQ exhibits immense promise as a solution, outperforming alternative methods with its distinct advantages. Furthermore, its potential for further adaptation and enhancement opens up new avenues for optimizing energy consumption and extending the lifespan of battery-powered IoT devices and sensors.

Keywords: IoT Communications, Error Control, Hybrid Automatic Repeat ReQuest, Incremental Redundancy, Energy Efficiency

Resumo

A rápida expansão dos sistemas da Internet das Coisas (IoT), que englobam uma vasta gama de dispositivos e sensores com uma duração limitada da bateria, veio realçar a necessidade crítica de soluções energeticamente eficientes para prolongar o tempo de vida operacional destes dispositivos alimentados por bateria.

Uma estratégia eficaz para reduzir o consumo de energia é minimizar a retransmissão de pacotes de dados em caso de erros de comunicação. Dentro da gama de potenciais soluções, os esquemas de comunicação Incremental Redundancy Hybrid Automatic Repeat reQuest (IR-HARQ) têm surgido como opções particularmente interessantes.

Este trabalho pretende responder a este desafio através do desenvolvimento de um simulador capaz de executar, analisar e validar vários testes envolvendo diferentes esquemas (H)ARQ. O objetivo principal é comparar o seu desempenho via múltiplas métricas, permitindo uma avaliação abrangente das suas capacidades.

O simulador proposto terá um elevado nível de configurabilidade, oferecendo diversos parâmetros ajustáveis em diferentes categorias para possibilitar a simulação de uma vasta gama de cenários. Esta adaptabilidade permitirá recriar várias situações do mundo real e explorar o comportamento de diferentes estratégias (H)ARQ em diversas circunstâncias.

Os resultados obtidos indicam que o IR-HARQ é uma solução muito promissora, superando os métodos alternativos com as suas vantagens distintas. Além disso, o seu potencial para mais adaptações e melhorias abre novos caminhos para otimizar o consumo de energia e prolongar a vida útil dos dispositivos e sensores IoT alimentados por bateria.

Palavras chave: Comunicações IoT, Controlo de Erros, Hybrid Automatic Repeat ReQuest, Redundância Incremental, Eficiência Energética

Acknowledgements

The completion of this dissertation would not have been possible without the support and encouragement of many individuals. I would like to extend my sincerest gratitude to the following people.

Firstly, I would like to express my heartfelt thanks to my parents and grandparents. Your unconditional love and support have been my source of strength and inspiration throughout my academic journey. Your encouragement and belief in me have made all the difference, and I am forever grateful for your sacrifices and hard work.

I would also like to express my gratitude to my friends. Your friendship and support have been invaluable, and I cannot thank you enough for always being there for me, especially during the most challenging times. I would like to extend an additional note of appreciation to my dear friends Cristiana, Francisco e Gonçalo for their unwavering support, motivation and kindness.

Finally, I would like to extend my deepest gratitude to my supervisor, Professor Nuno Almeida. Your expertise, guidance, and support throughout the entire process of working on this dissertation have been invaluable. Your constructive feedback and encouragement helped me stay focused and motivated, and I am grateful for your willingness to make time for me despite your busy schedule.

Thank you all for your support, encouragement, and inspiration. I could not have done it without you.

Sérgio Silva

"There is a theory which states that if ever anyone discovers exactly
what the Universe is for and why it is here,
it will instantly disappear and be replaced
by something even more bizarre and inexplicable."

Douglas Adams

Contents

List of Figures

List of Tables

Abbreviations

3GPP	3rd Generation Partnership Project
5G	5th Generation
ARQ	Automatic Repeat Request
AWGN	Additive White Gaussian Noise
BCH	Bose–Chaudhuri–Hocquenghem
BER	Bit Error Rate
BMS	Binary-input Memoryless Symmetric
BPSK	Binary Phase Shift Keying
CC-HARQ	Chase Combining Hybrid Automatic Repeat Request
CRC	Cyclic Redundancy Check
FEC	Forward Error Correction
GE	Gilbert-Elliott
HARQ	Hybrid Automatic Repeat Request
IEEE	Institute of Electrical and Electronics Engineers
IoT	Internet of Things
IR-HARQ	Incremental Redundancy Hybrid Automatic Repeat Request
M2M	Machine to Machine
mMTC	Massive Machine Type Communications
MRC	Maximal Ratio Combining
QPSK	Quadrature Phase Shift Keying
RSC	Recursive Systematic Convolutional
SNR	Signal to Noise Ratio
URC	Ultra Reliable Communications
URLL	Ultra Reliable Low Latency

Chapter 1

Introduction

This chapter presents the scope of the dissertation, as well as the assumptions and motivations for this work. The structure of the document is detailed at the end of the chapter.

1.1 Context and Motivation

In this day and age, communication systems are essential to everyday life for the general population. However, over the history of its development, major advances have focused fundamentally on getting higher data rates.

While this trend is predicted to continue, the next generation of mobile networks is expected to support a much larger number of devices with much stricter requirements [1]. These requirements include not only device density, as in the case of Massive Machine Type Communications (mMTC) in 5G, but also latency and reliability in Ultra Reliable Low Latency (URLL) in 5G.

One of the main beneficiaries and motivators for these changes is the Internet of Things (IoT) concept, with a substantial impact on the field of telecommunications in recent years. With Ericsson [2] predicting an estimated 5 billion IoT devices connected by the year 2025, IoT is set to be one of the largest components in the mobile networks of the very near future.

However, the fast expansion and inherent diversity of IoT devices introduce some key challenges and requirements. One of these issues is the support for low power operation as most IoT devices are battery powered, used to monitor remote or not easily accessible places, such as bridges [3] or large indoor areas. The inaccessibility of these places makes regular recharging or replacing of device batteries unfeasible, and, as such, the batteries would need to last years and even decades.

One possibility to reduce power consumption is minimizing the retransmission of packets. Packet transmission or communication, in general, would be one of the heaviest power consumers and, therefore, one of the critical problems to be targeted for energy consumption reduction.

To overcome the challenge of minimizing packet retransmission, the chosen strategy was the use of Incremental Redundancy Hybrid Automatic Repeat reQuest (IR-HARQ) communication schemes as the basis for sensor and device communications.

1.2 Objective

The work relative to this dissertation aims to set up a simulated testing environment for sensor communications. This main objective can be subdivided into multiple parts:

- Study the context and technologies related with low energy consumption in IoT devices.
- Evaluate the possibility of achieving enhanced low-power transmissions using novel ARQ schemes, namely Incremental Redundancy HARQ scheme.
- Related with analysis and evaluation of ARQ schemes in sensor communications:
  - Develop a simulated testing environment.
  - Assess energy efficiency gains and other metrics of IR-HARQ when compared with previous schemes (ARQ, HARQ), across various scenarios.

1.3 Document Structure

This document is composed of 6 chapters.

Chapter 1 is the introduction, aimed at defining the work's context, motivation and objectives.

Chapter 2 presents some fundamental aspects needed to understand the proposal better. As such, it introduces ARQ, HARQ and IR-HARQ communications schemes as well as presents some Forward Error Correction (FEC) codes.

Chapter 3 presents the problems related to sensor networks and proposed solutions.

Chapter 4 explains the development process and includes metrics, variables and a characterization of the schemes.

Chapter 5 shows the obtained results from each scenario, as well as their analysis and conclusions.

Chapter 6 concludes the document, detailing the main conclusions, contributions as well as future work.

Chapter 2

Background and State-of-the-Art

In this chapter, some works regarding the use of the various ARQ types and their performance are presented, as well as their results.

In order to understand the problem at hand, the proposed work and its implications, some essential knowledge on the subject is needed.

2.1 Channel Models

2.1.1 Additive White Gaussian Noise

The Additive White Gaussian Noise (AWGN) channel model is meant to represent, in a simple way, the effects of noise in a given channel.

This model adds a random signal to the channel with a constant spectral density over the entire frequency range, and it follows a normal distribution whose mean is 0 and variance is σ^2.

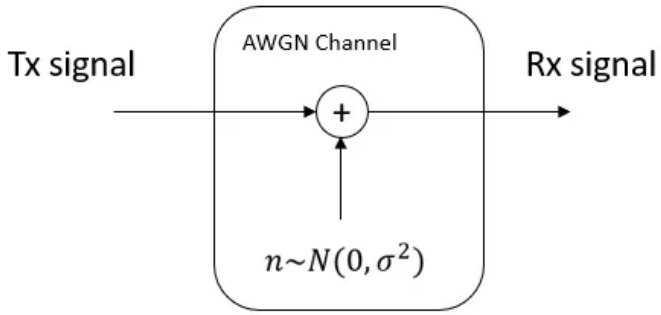

Figure 2.1: AWGN channel link. Reprint from : [4]

2.1.2 Gilbert-Eliott

The Gilbert-Elliot channel model, often referred to as the Gilbert model, is a widely employed framework in the field of communication theory [5] [6]. This model serves as a valuable tool for

characterizing and understanding the behaviour of communication channels that exhibit burst error patterns. By employing a two-state Markov chain, the Gilbert-Elliot channel model effectively models the transition between periods of reliable transmission (termed the "good" state, denoted as G) and intervals with a higher error rate (referred to as the "bad" state, denoted as B).

To depict this model, it is crucial to delve into the key components. Firstly, the model encompasses two primary states: good (G) and bad (B). These states represent distinct conditions of the communication channel. The "good" state signifies a phase in which the channel operates reliably with a low probability of errors, while the "bad" state reflects a period of increased vulnerability to errors and disruptions.

The crux of the Gilbert-Elliot channel model lies in its characterization of the transitions between these two states. The transitional probabilities are defined as P_{BG} for the transition from the bad state to the good state and P_{GB} for the transition from the good state to the bad state.

A complete diagram depiction of the Markov chain can be seen in Figure 2.2:

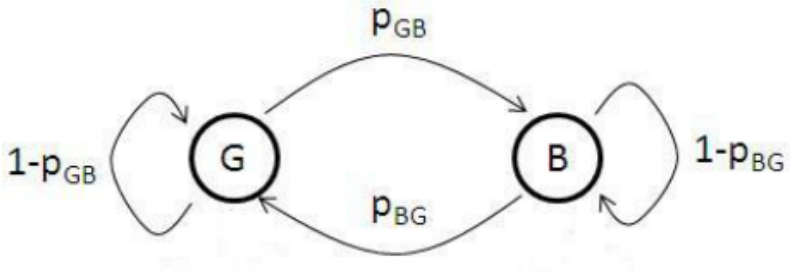

Figure 2.2: Two-state Gilbert-Elliot model of a bursty communication link. Reprint from : [7]

2.2 Forward Error Correction

The most important types of error correction codes are block and convolutional codes. The main difference between them is the memory of the encoder. In block codes, each operation is independent of previous encoding operations. Meanwhile, convolutional codes' output depends not only on the current input but also on a given number of past message blocks [8].

The choice of one or multiple error correction codes is an integral part of the plan and development of this dissertation, and as such, some error correction codes will be characterized.

2.2.1 Reed Solomon Codes

Reed Solomon codes are a subset of Bose–Chaudhuri–Hocquenghem (BCH) codes and are linear block codes.

A Reed-Solomon code generates codewords composed of data symbols and parity symbols, as shown in Figure 2.3. Within each codeword, `k` is the number of data symbols, and 2t is the number of parity ones. This makes each codeword have `n` symbols in total. A codeword with these values is capable of correcting `t` errors in a codeword where $2t = n - k$.

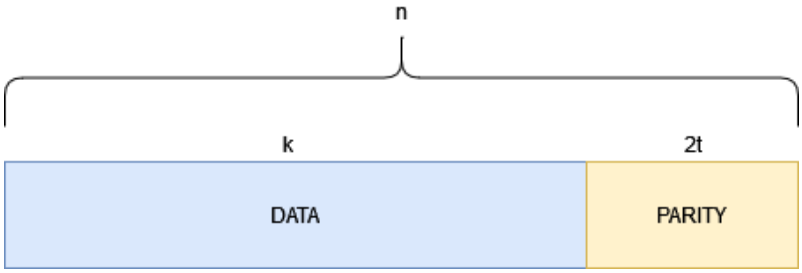

Figure 2.3: Typical Reed-Solomon codeword. Adapted from: [9]

Reed-Solomon codes are based on finite field arithmetic. These finite fields have the property that arithmetic operations on the field elements have a result also on the field. These fields are also known as Galois fields[9][10][11].

2.2.1.1 Generator Polynomial

All Reed-Solomon codewords are obtained using a special polynomial. All valid codewords are divisible by the generator polynomial. The general form of this polynomial is [9]:

$$g(x) = (x - \alpha^{i})(x - \alpha^{i+1})...(x - \alpha^{i+2t}) \tag{2.1}$$

And the codeword is obtained using the following:

$$c(x) = g(x).i(x) \tag{2.2}$$

where $g(x)$ is the generator polynomial and $i(x)$ is the information block.

2.2.1.2 Advantages

Reed-Solomon decoders correct the entire codeword and therefore, they provide great resistance to burst errors. This is a substantial advantage due to the relative commonality of burst errors in wireless communications.

2.2.2 Turbo Codes

Turbo codes are a subset of convolutional codes that generate code words as the convolution of the message and the impulse response of a shift register. An input bit has influence over multiple output bits, therefore spreading the original information.

2.2.2.1 Turbo Encoding

The Turbo-Code encoder is characterized by a parallel concatenation of two Recursive Systematic Convolutional (RSC) codes [12].

A typical Turbo encoder has the following structure:

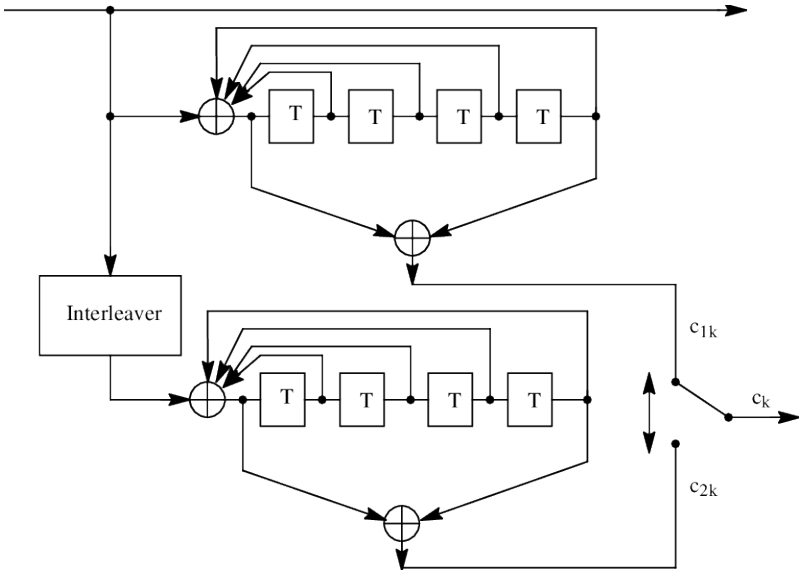

Figure 2.4: Turbo Code Encoder. Reprint from: [13]

Each input message is run through two different encoders separated by an interleaver, effectively using two encoders to encode data. The interleaver scrambles the input data before inputting it into the second encoder, so the second codeword is different from the first. The effect of this is a higher probability of a codeword having a higher Hamming weight.

2.2.2.2 Advantages

The main advantage of Turbo codes is their ability to achieve a low bit error ratio (BER) at low SNR, making them ideal for low-power communications [14].

2.2.3 Polar Codes

Polar codes, as defined in [15], are linear block codes that are able to achieve the capacity of binary-input memoryless symmetric (BMS) channels. The encoding and decoding of polar codes can be done with low complexity.

The construction of polar codes relies on the recursive application of invertible linear transformations, which split the original binary-input channel into a number of bit subchannels.

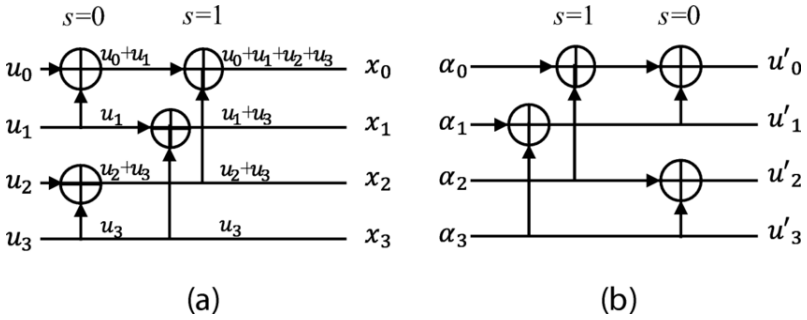

Figure 2.5: Polar code encoding and decoding example for N = 4. (a) Encoding. (b) Decoding. Reprint from: [16]

2.2.3.1 Advantages

Polar codes are capable of reaching channel capacity for symmetric channels, including binary symmetric channel [17]. Polar codes have a better performance in the case of shorter messages when compared to other codes [18].

2.3 (H)ARQ Schemes

Firstly, we must understand why IoT traffic differs from regular undifferentiated traffic. The three major challenges in IoT, specifically in Machine-to-Machine (M2M) communications, according to [19] are:

- **Extremely Short Packet Size:** Most sensors in IoT systems only connect sporadically and transmit very small packets. This differs from regular downlink traffic that is expected of services such as video streaming. As such, protocols and schemes must be adapted to this small packet size, often by reducing overhead caused by multiple transmissions in many small packets as opposed to the regular transmissions of big packets.

- **Energy Efficiency:** IoT devices are often battery-powered and, consequently, reducing energy consumption by minimizing retransmissions helps prolong battery life, possibly for multiple years depending on the device. Reducing retransmissions also decreases the mutual interference that these devices may experience if placed in close enough proximity, thus improving overall network quality.

- **Diverse Performance Requirements:** Though most IoT devices benefit from the tradeoff between low power consumption and other factors such as delay and error probability, some devices, like the ones implementing Ultra Reliable Communications (URC), which require extremely low outage probability and low delivery delays, cannot afford such a cost. Thus, energy efficiency and performance need to be balanced according to the type of network being developed.

After acknowledging the challenges presented by this type of network, a solution must be proposed to improve the efficiency aspect of the network.

The next step is understanding ARQ and the combination of ARQ with forward error correction, known as Hybrid Automatic Repeat Request(HARQ).

The addition of forward error correction codes improves reliability in transmission by making the information being transmitted, in our case, the packets, resilient to random errors.

Although this definition is a stepping stone to better understanding the processes, one must also understand the algorithm and operation of each protocol and its advantages and disadvantages.

For this proposal, the solution to improve energy efficiency is to use Incremental Redundancy Hybrid Automatic Repeat ReQuest (IR-HARQ) as a scheme of retransmission and forward error correction.

Effectively, IR-HARQ is a topic that, in recent years, has been receiving attention from several authors, as can be seen in [20] [21].

To evaluate the gains that IR-HARQ offers, it must be compared to ARQ and other variations of it. Before comparing, however, each HARQ process must be defined according to its mode of operation [19]:

- **ARQ:** Only data packets are sent. If errors are detected, the packet is discarded.
- **Type-I:** Both data and redundancy are sent in the same packet. The receiver discards the packet if the decoding fails. (Fig.2.6).
- **Type-II:** Data and redundancy are sent in two transmissions. Each received version of a specific redundancy is combined with every received version of itself. (Fig.2.7).
- **Incremental Redundancy (IR):** The data and redundancies are divided into multiple transmissions, which are sent in successive transmission attempts. (Fig.2.8).

A concise explanation and visual representations are present in the following sections to better clarify and explain.

2.3.1 HARQ - Type I

Data and redundancy are sent in the same packet in each transmission round. Additionally, when the maximum number of transmissions M has been achieved, or the packet has been successfully decoded, the transmitter stops sending that packet. The receiver makes the decisions only based on the last packet received and ignores any earlier packets.

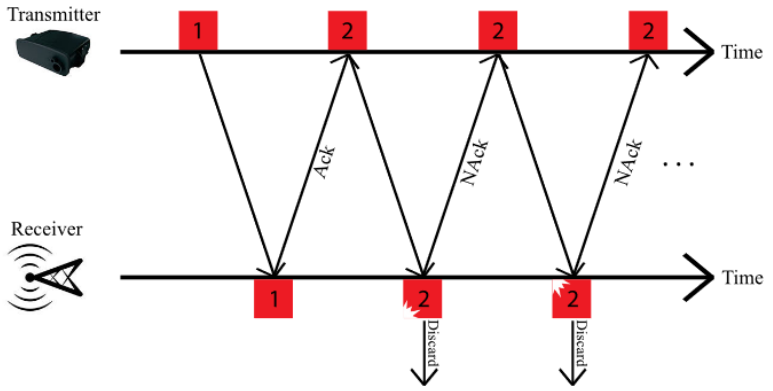

Figure 2.6: The setup for HARQ - Type I protocol. Reprint from: [22]

2.3.2 HARQ - Type II

The data packet and redundancy packet are divided into two transmissions. The redundancy is used to attempt to correct the data packet. Combining of different data and redundancy packets is possible as seen in Figure 2.7.

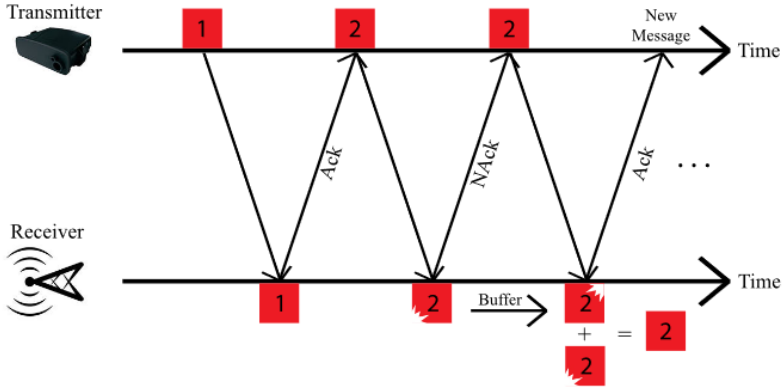

Figure 2.7: The setup for HARQ - Type II protocol. Reprint from: [22]

2.3.3 IR-HARQ

The principle behind IR-HARQ is that the transmission is split between data and multiple redundancies, each redundancy larger than the previously sent.

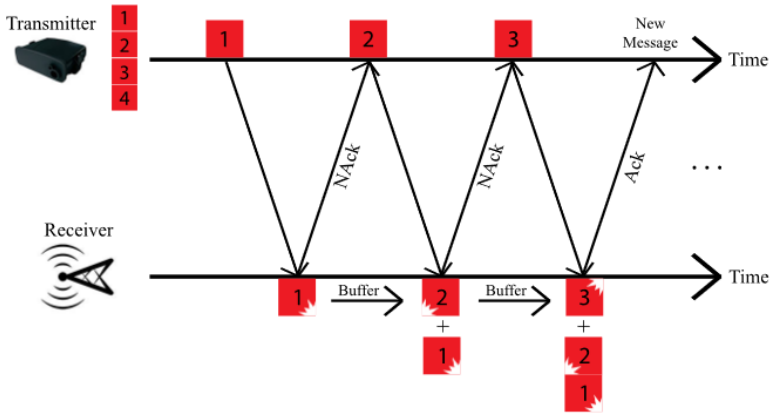

Figure 2.8: The setup for IR-HARQ protocol. Reprint from: [22]

2.4 State-of-the-art

2.4.1 Energy vs Outage Probability

In [22], the authors develop relatively low complexity power allocation algorithms, as well as provide a closed-form approximation for the outage probability of the IR-HARQ protocol. After developing power allocation algorithms, the authors compare various metrics of ARQ, CC-HARQ and IR-HARQ transmission schemes.

Figure 2.9 shows the variation of transmit power ρ_i in each round versus the outage probability target ϵ, for a maximum of two transmissions (i=1,2).

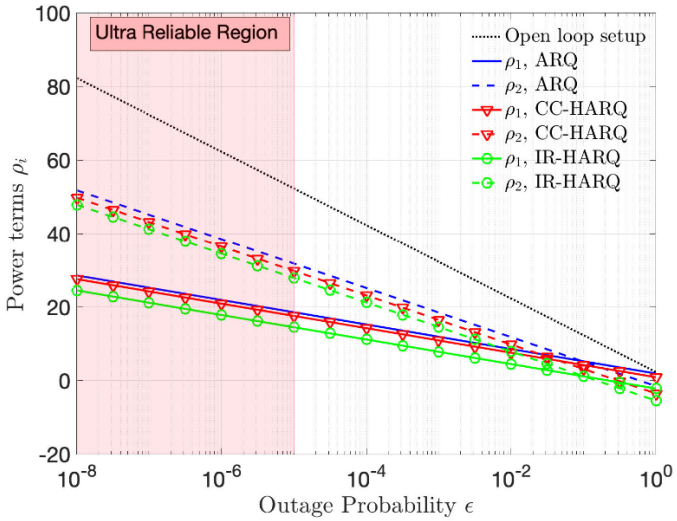

Figure 2.9: Transmit power in each round to achieve a target outage probability. Reprint from: [22]

One observation that can be made is that the IR-HARQ protocol gives the best results in terms of power saving. Furthermore, in the case that the first round (i=1) is successful we can observe

savings of 30 to 35 dB (for ARQ, CC-HARQ and IR-HARQ) in relation to the open loop setup when $\varepsilon = 10^{-5}$, which represents the start of the Ultra-Reliable Region. [1]

Figure 2.10 shows the average power consumed for each protocol and two different values in the number of maximum possible transmissions (M=2,3).

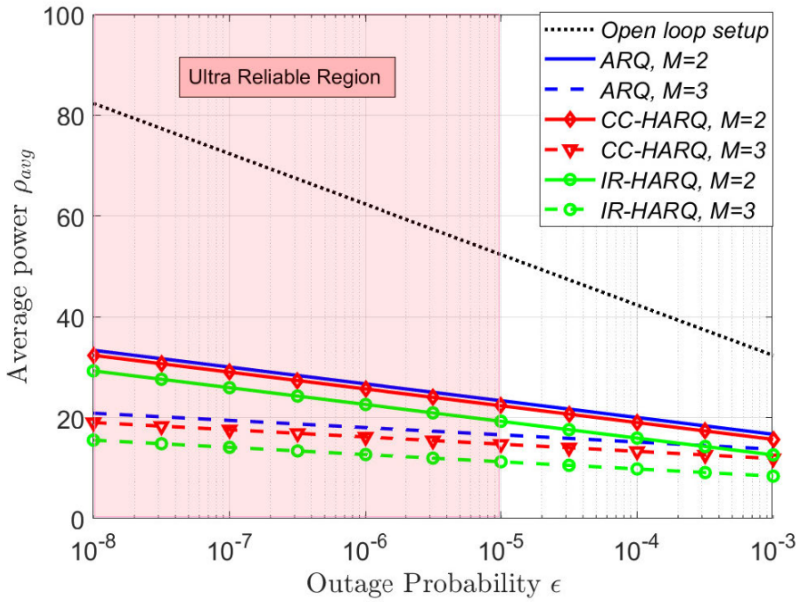

Figure 2.10: Average power required to achieve a target outage probability. Reprint from: [22]

One conclusion that can be taken from figure 2.10 is that there is a significant amount of saved power when comparing the open loop setup with any of the protocols. In addition to this, when comparing these results with the results previously shown in figure 2.9, we can observe that as the number of transmissions increases, more power is saved on average.

Finally, in figure 2.11 the maximum power expenditure in the worst-case scenario is shown. This plot assumes all transmissions were exhausted.

[1] 3GPP defines URLLC requirements for a payload of 32 bytes and 99.999% reliability.

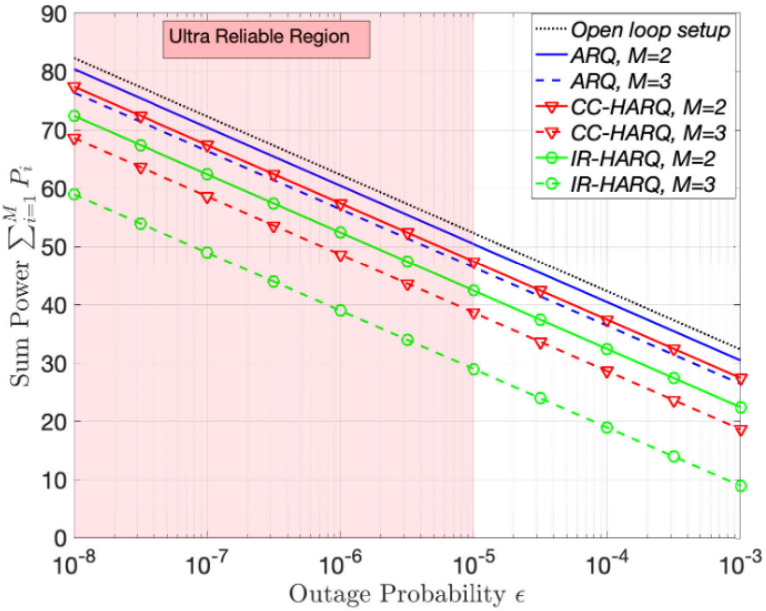

Figure 2.11: Maximum power that will be spent to achieve a target outage probability. Reprint from: [22]

In figure 2.11 we can again observe the significant savings over an open loop setup, especially in the case of IR-HARQ where, when M=3, showed savings of 20 dB. Another relevant aspect is that, due to not benefitting from combining gains, the ARQ protocol doesn't significantly improve when the number of transmissions increases.

In [19], the authors provide a performance comparison between various HARQ schemes, considering short packets and energy constraints.

Figure 2.12 shows the outage probability for the average consumed energy. As expected, all HARQ schemes outperformed the baseline open loop system due to the retransmissions. Additionally, IR-HARQ has the best performance in outage probability when compared to all other schemes.

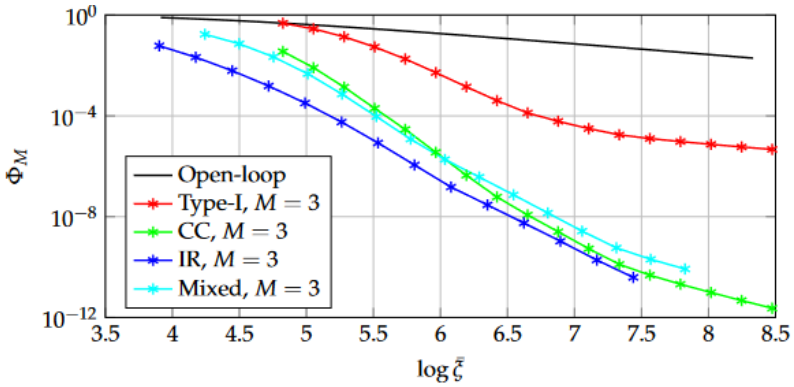

Figure 2.12: Outage probability Φ_M vs. average consumed energy $\bar{\zeta}$. Note that $\bar{\zeta}$ is represented on a logarithmic scale. Reprint from: [19]

Additionally, in [19] the authors compare the energy gains of Type-II HARQ schemes when compared to Type-I HARQ.

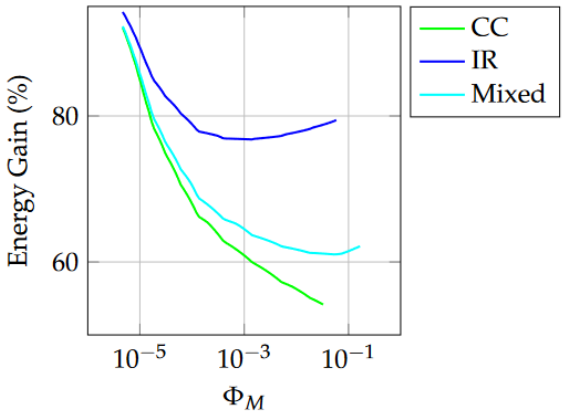

Figure 2.13: Energy gap of CC, IR, and mixed HARQ with respect to Type-I HARQ vs outage probability Φ_M. Reprint from: [19]

From this figure, we can conclude that overall Type-II HARQ provides significant energy gains when compared to Type-I HARQ, with gains from around 50% to as high as 90%. As expected, the IR scheme obtains the highest gain for all outage probabilities.

2.4.2 Throughput vs Signal to Noise Ratio

In [23], the authors propose IR-HARQ schemes for systematic polar codes and compare the proposed schemes with the HARQ scheme in the high-quality-of-service mode of the IEEE 802.15.6-2012 standard.

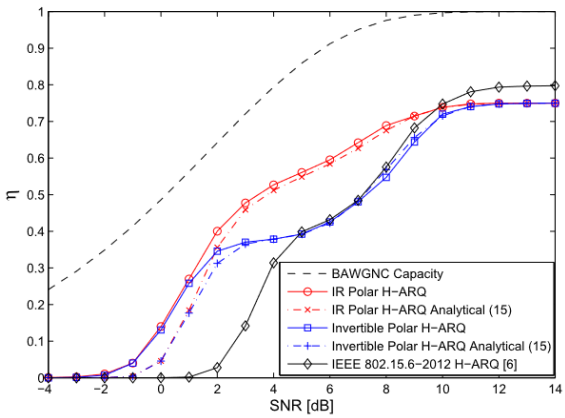

Figure 2.14: Throughput performance of the proposed HARQ schemes in comparison with IEEE 802.15.6-2012 HARQ (N = 128 and R = 1/2) and the theoretical approximation. Reprint from: [23]

This figure shows an advantage of the HARQ scheme based on invertible polar codes at low SNR of about 4 dB when compared to the IEEE standard scheme. At high SNR, however, the performance is comparable. The IR-HARQ scheme also achieves a 4 dB advantage at low SNR.

Each of these 3 works shows a clear tendency for IR-HARQ to have advantages over other schemes when transmitting and retransmitting at low SNR, as well as having significantly lower power consumption.

Chapter 3

Sensor Networks: Related Problems and Proposed Solutions

Sensor networks have emerged as a pivotal component of the Internet of Things (IoT) ecosystem, enabling the collection and transmission of real-time data from various physical environments. These networks consist of interconnected sensors that gather information about the surrounding environment and communicate the data to a central location or other networked devices. While sensor networks offer numerous advantages, they also present challenges that must be addressed to ensure their effective and efficient operation. This chapter examines the related problems encountered in IoT sensor networks and proposes potential solutions to mitigate their impact.

3.1 Related Problems

3.1.1 Sensor Node Deployment and Coverage

One critical issue in IoT sensor networks is the optimal deployment and coverage of sensor nodes [24]. The positioning of sensor nodes significantly influences the accuracy and reliability of the data collected. Challenges arise when determining the appropriate number of nodes, their spatial distribution, and their power constraints to maximize coverage and minimize redundancy.

Insufficient sensor coverage may lead to data gaps or incomplete monitoring, impairing the network's overall functionality. To address this problem, advanced algorithms and optimization techniques can be employed to optimize sensor node deployment and improve coverage efficiency, ensuring comprehensive data collection across the monitored area.

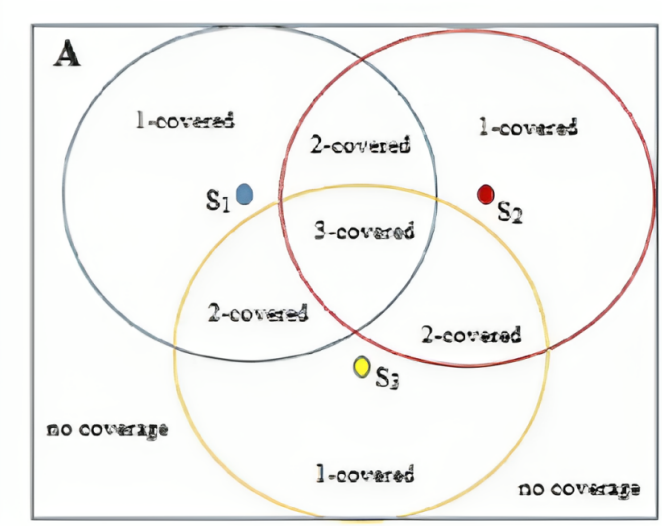

Figure 3.1: Various Levels of Coverage In a Wireless Sensor Network. Reprint from: [25]

3.1.2 Energy Efficiency and Battery Life

Energy efficiency is a significant concern in IoT sensor networks due to the limited power resources of sensor nodes. These nodes are often battery-powered and are not connected to any energy source. There is only a finite source of energy, which must be used most efficiently for processing and communication [26] [27]. Prolonged network lifetime is crucial to avoid frequent node replacements, which can be costly and disruptive as these sensors may be deployed in inaccessible or hard-to-access places, as is the scenario seen in Figure 3.2. To address this challenge, advanced techniques such as ARQ schemes, specifically Incremental Redundancy HARQ, can optimize energy consumption and extend battery life.

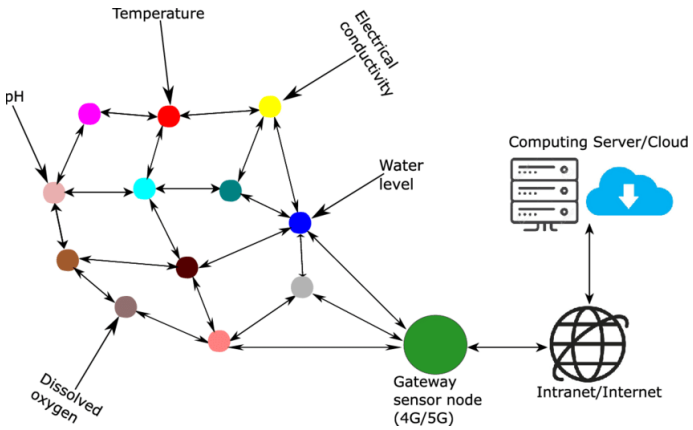

Figure 3.2: Example of Wireless Sensor Network deployment on a mine. Reprint from: [28]

By utilizing Incremental Redundancy HARQ, sensor nodes can efficiently transmit various degrees of redundancies rather than retransmitting a single redundancy or another whole data

packet. This approach reduces the energy overhead of retransmissions, as only the redundancy is transmitted.

In addition to ARQ schemes, other energy-saving techniques can be employed, such as duty cycling and data aggregation. Duty cycling involves alternating between active and sleep states, allowing sensor nodes to conserve energy during idle periods. Data aggregation involves combining multiple data packets into a single packet before transmission, reducing the overall amount of transmitted data and minimizing energy consumption.

Moreover, integrating energy harvesting methods, such as solar energy, can supplement or replace battery power, ensuring a sustainable energy source for the sensor nodes. By leveraging a combination of ARQ schemes like Incremental Redundancy HARQ, duty cycling, data aggregation, and energy harvesting, IoT sensor networks can significantly enhance energy efficiency, prolong battery life, and reduce the overall environmental impact of the network operation.

3.1.3 Data Security and Privacy

Data security and privacy are paramount concerns in IoT sensor networks, as they handle sensitive information from diverse domains, including healthcare, transportation, and industrial applications. These networks are vulnerable to various security threats, such as unauthorized access, data tampering, and privacy breaches, due to the high heterogeneity and the large scale of potential networks [29]. Ensuring data integrity, confidentiality, and availability is critical to maintaining user trust and protecting against malicious activities. Advanced cryptographic techniques, secure communication protocols, and access control mechanisms can be implemented to safeguard the data transmitted and stored within the network. Moreover, privacy-enhancing technologies, including data anonymization and differential privacy, can be employed to protect the privacy of individuals whose data is collected by the sensor network.

3.1.4 Scalability and Network Management

Scalability poses a significant challenge in IoT sensor networks, especially as the number of connected devices and data volume grows exponentially. As the network expands, the management of sensor nodes, data storage, and processing becomes increasingly complex. Efficient network management techniques are required to handle the scalability issue, including distributed data storage, load balancing mechanisms, and scalable routing protocols. Furthermore, intelligent data analytics and machine learning algorithms can be employed to extract meaningful insights from the vast amounts of data generated by the sensor network, facilitating efficient decision-making processes.

3.2 Proposed Solutions

IoT sensor networks have revolutionized data collection and monitoring capabilities, enabling various applications across various domains. However, the deployment and operation of these networks are not without challenges. This chapter discussed the related problems encountered in IoT

sensor networks, including sensor node deployment, energy efficiency, data security and privacy, scalability, and data reliability. Proposed solutions were presented, highlighting the potential of optimization algorithms, energy-efficient techniques, security measures, and network management strategies.

The main focus of this dissertation lies in trying to study energy efficiency as, in addition to these solutions, adopting ARQ schemes, specifically Incremental Redundancy HARQ (IR-HARQ), can significantly enhance data reliability and energy efficiency in IoT sensor networks. HARQ combines forward error correction with retransmission-based error recovery mechanisms to mitigate the impact of packet losses and transmission errors. By utilizing IR-HARQ, sensor nodes can send data in the form of smaller, incremental packets of redundancy, allowing for efficient retransmissions and reduced overhead.

Chapter 4

Simulator Implementation of ARQ Schemes

This chapter presents the implementation of the simulator used for ARQ schemes. The practical evaluation and analysis of ARQ schemes necessitate the availability of a simulation framework capable of accurately modelling their behaviour and performance characteristics. Thus, this chapter focuses on the development and implementation of the simulator, the various metrics obtained, the variables that can be modified, and a comprehensive explanation of every used scheme.

4.1 First Considerations and Tests

The project's initial phase entailed careful deliberation concerning selecting an appropriate platform for developing the simulator. Following discussions and evaluations of various alternatives, the decision was reached to employ MATLAB [30] as the preferred platform. The decision to employ MATLAB was based on familiarity and extensive online documentation.

After selecting the simulator platform and searching for a viable code base, a set of pseudocode comprising a partial implementation of certain desired features was discovered. This code [31], although not functional, was deemed suitable to initiate the establishment of a framework for the project.

Subsequently, the initial code underwent significant enhancements, encompassing error rectification and incorporating implementations of the forthcoming schemes and desired metrics. To verify that each distinct scheme and variable did not alter the accurate simulation of transmission errors, the Channel Bit Error Ratio (BER) was calculated for each configuration. This examination and fine-tuning of the simulator were essential since the Channel BER should remain invariant across all the diverse configurations, as the scheme must not influence the error rate during transmission. One such comparison of Channel BER among schemes is shown in figure 4.1:

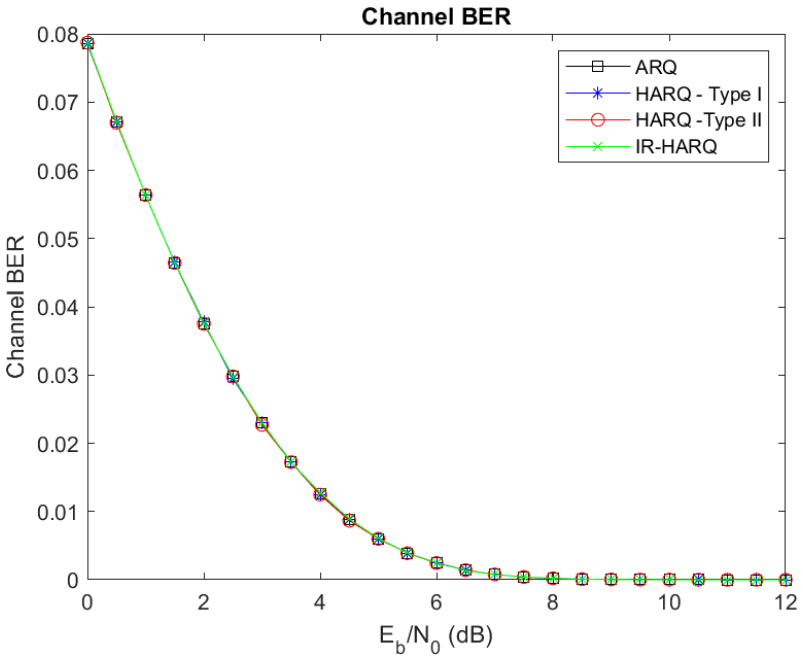

Figure 4.1: Example of the Channel BER plot when well calibrated.

As shown in figure 4.1, all the plots for the various schemes overlap, showing the simulator's correct implementation and functioning.

4.2 General Description of Implemented ARQ Schemes

In this simulator, four different schemes were implemented. A brief description of each is explained hereafter:

- **ARQ** - The simplest to implement. If an error is detected in data transmission, it resends the same packet.
- **HARQ - Type I** - Adds Forward Error Correction (FEC) redundancy to the end of a regular data packet and sends this new packet all at once. If there are errors in data transmission, it attempts to correct them using the appended redundancy. If this redundancy is insufficient, it sends a new, equal packet.
- **HARQ - Type II** - The same redundancy as in the previous scheme is used. The transmission of data and redundancy, however, is split between two packets. If the data packet has errors at reception, the redundancy is sent in the following transmission and used to try to correct the original message.
- **IR-HARQ** - Has R levels of redundancy (R >= 2), with level 1 being the weakest and R the strongest. Therefore, for each data packet, there are 1+R different packets that can be transmitted. For the case of R = 3, if the data packet has errors at reception, then level 1 redundancy is sent in the following transmission and used to try to correct the original

message. If this fails, level 2 is sent. This same idea applies until level R is sent as the final redundancy.

4.3 Choice of Metrics and Variables

After successfully implementing the intended schemes, the subsequent stage involved the selection of appropriate variables that would be modified to formulate a set of diverse scenarios. In addition, specific metrics to be monitored and compared among these distinct scenarios were discussed and chosen.

4.3.1 Metrics

To define the chosen metrics, a set of internal parameters and values had to be specified. This set is shown in tables 4.1 and 4.2.

Table 4.1: Simulator Internal Parameters

Total Number of Data Packets	N	1000
Data Bits per Packet	D	980
Total Number of Data Bits to Transmit	L_d	980000
Maximum Attempts per Packet	M	3 or 8

Table 4.2: Simulator Internal Values

(Re)Transmissions of Packet i	Tx_P_i	[1,M]
Total Number of Bits (Re)Transmitted	L_{tx}	[L_d,M*L_d]
Total Number of Failed Packets	F	[0,N]
Total Number of Data Bits Recovered	$L_{d,rx}$	[0,L_d]

4.3.1.1 Packet Loss Ratio

The initial metric selected for analysis in the context of the transmission simulation was the measurement of "Packet Loss Ratio". This particular metric is defined as the quantification of the number of data packets that failed to successfully reach the destination after undergoing the maximum allowable number of transmission attempts.

This metric is critical in monitoring and evaluating different HARQ schemes by assessing their respective abilities to minimize the occurrence of complete data loss.

$$Packet\ Loss\ Ratio = \frac{Total\ No.\ Failed\ Packets}{Total\ No.\ Data\ Packets} = \frac{F}{N} \tag{4.1}$$

4.3.1.2 Average Transmissions per Packet

The metric of "Average Transmissions per Packet" was chosen as another crucial measure for analysis within the simulation. This metric is characterized by quantifying the average number of transmission attempts required for a data packet to reach its intended destination successfully.

By evaluating the average transmissions per packet, we are able to verify the capabilities of varying schemes in terms of minimizing the transmission attempts needed to achieve successful delivery. This metric also needs to be assessed in terms of the functioning of the various different schemes, as several of them do not transmit the same quantity of information within the same number of transmissions.

$$Avg.Transmissions = \frac{\sum_{i=1}^{N}(Re)Transmissions\ of\ Packet_i}{Total\ No.\ Data\ Packets} = \frac{\sum_{i=1}^{N} Tx\_P_i}{N} \tag{4.2}$$

4.3.1.3 Data Transmission Efficiency

The next metric established for analysis was "Data Transmission Efficiency." This metric is defined as the comparison between the size of an individual data packet and the aggregate number of bits transmitted during all attempts to successfully transmit the original data. Notably, this metric assumes a zero value if the specific packet fails to reach the destination, as it signifies the absence of useful data bits in such instances.

This metric allows for comparing different schemes in terms of how much the schemes effectively utilize the communication channel for successful data transmissions. A higher data transmission efficiency value indicates a greater proportion of the channel's capacity dedicated to transmitting useful data, leading to increased throughput and reduced resource wastage.

$$Data\ Efficiency = \frac{Total\ No.\ Data\ Bits\ Recovered}{Total\ No.\ Bits\ (Re)Transmitted} = \frac{L_{d,rx}}{L_{tx}} \tag{4.3}$$

4.3.1.4 Normalized Energy

The metric of "Normalized Energy" involves the evaluation of energy consumption in the transmission of a packet i ("Consumed_Energy$_i$"), be it successful or not, by comparing it to a predefined reference amount of energy expended in the ideal or perfect transmission of a data packet ("Reference_Energy"). This metric serves as a quantitative measure for assessing the efficiency and effectiveness of different schemes in terms of energy utilization. By normalizing the energy consumed during successful packet transmissions against a reference value, we can evaluate the relative energy efficiency of each scheme.

This metric allows for evaluating how, at each point, a given scheme's energy consumption deviated from an ideal scenario. Higher normalized energy values suggest a less efficient energy utilization, indicating potential areas for energy-saving improvement.

$$Normalized\ Energy = \frac{1}{N} * \sum_{i=1}^{N} \left(\frac{Consumed\_Energy_i}{Reference\_Energy} \right) \tag{4.4}$$

The analysis for this metric can be done from two different perspectives, each considering different parts of the system.

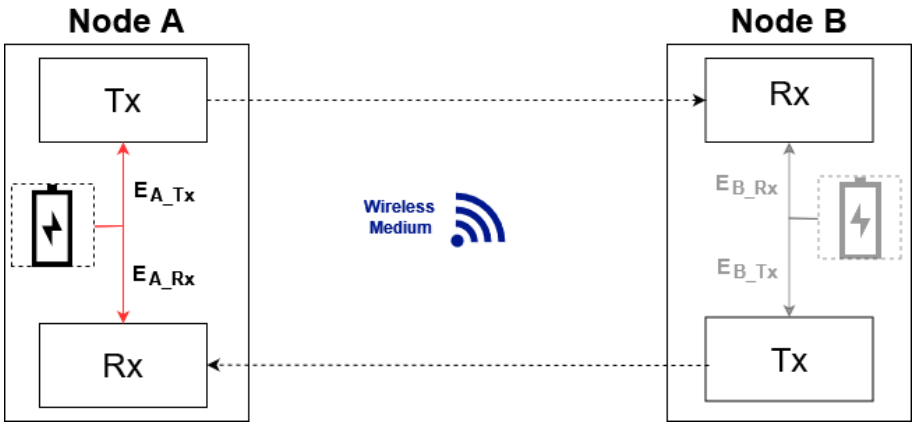

Figure 4.2: Energy from the perspective of Node A

Analysis from the perspective of a single node: As can be seen in figure 4.2, the first perspective is that of a single node, in our case, the main transmitter. For the energy analysis from this perspective, only the energy from transmission from node A and reception for node A are considered.

Figure 4.3: Energy from the perspective of both Nodes A and B

Analysis from the perspective of a Transmitter-Receiver pair: Figure 4.3 shows the second perspective, that being of the full pair of Transmitter and Receiver. Both the energies for transmission and reception from nodes A and B are considered in this case.

4.3.2 Variables

4.3.2.1 E_b/N_0 Levels

In evaluating different HARQ schemes, data points are collected at varying energy-to-noise ratio (E_b/N_0) values. This deliberate approach aims to comprehensively monitor the progression and behaviour of various metrics across different channel conditions.

The choice of E_b/N_0 is also a crucial part, as different values allow insight into different qualities or shortcomings of each scheme. By systematically capturing data at multiple E_b/N_0 levels, we can effectively investigate the impact of changing signal-to-noise ratios on the performance of the schemes. By collecting data at high E_b/N_0 values, where the received signal is relatively stronger compared to noise, the performance in relatively optimal conditions can be analysed. Similarly, data collection at lower E_b/N_0 values, where noise becomes more dominant, provides insights into the schemes' robustness and resilience in poor channel conditions.

4.3.2.2 Maximum Allowed Transmissions

A second variable is the maximum number of allowed transmissions (M). This determines the number of total attempted transmissions a packet is allowed before being considered a failed transmission. During the tests, the value was set at two different values: M = 3 and M = 8. The smaller values allow for observing how the metrics react to a smaller number of total data packets in the case of HARQ - Type II and IR-HARQ. In opposition, the higher values theoretically allow for greater success, as these schemes have more chances for combining the various data and redundancy packets received if combining is used.

4.3.2.3 Receive and Transmit Energy Factors for each node

When considering the "Normalized Energy" metric, one variable to consider is the degree to which each transmission and reception affects the energy consumption. As such, the creation of variables for the energy consumption factors of each node's reception and transmission allows for the two different perspectives presented earlier, as well as different consumptions of each part of the system in relation to the reference value.

4.3.2.4 Use of Code Combining

Another noteworthy variable that was taken into consideration in this study is the utilization of Code Combining in HARQ - Type II and IR-HARQ protocols. The experimentation involved two situations: one where no combining of the different received data packets and redundancy packets was performed, and another where all received data and redundancy packets were combined with the aim of enhancing the success rate of message correction.

In the first situation, the received packets were treated independently without any attempt to combine them. This approach allows for a straightforward evaluation of the system's performance without the influence of combining techniques. On the other hand, the second situation involved

the merging of all data packets and all redundancy packets. By employing code combining, it is expected that the success rate of error correction would be augmented.

4.3.2.5 Modulation

In the context of modulation analysis, two key variables considered in this study are Binary Phase Shift Keying (BPSK) and Quadrature Phase Shift Keying (QPSK). These modulation schemes were chosen to investigate their respective impacts on the system performance and transmission quality.

Most of the study was conducted in BPSK, but all scenarios were also run in QPSK, as is to be seen in Chapter 5.

4.3.2.6 Channel Type

The primary focus of our research centred on the evaluation and analysis of communication systems under the influence of the AWGN channel model. However, it's worth noting that comparisons using a Gilbert-Elliott model were made and their results analysed.

4.4 Detailed Characterization of ARQ/HARQ used schemes

One of the first details to mention is that of FEC symbols. These can be converted to bits in a ratio of eight bits to one symbol.

When characterizing the used schemes, one of the first things to take into account is the FEC code used. In the case of this dissertation, all results were obtained using Reed-Solomon codes with varying degrees of redundancy, namely three levels: High, Medium and Low:

- **High Redundancy:** The highest level of redundancy entailed a coding rate of 0.4824, meaning only 48.24% of a packet was used for data. This resulted in 123 symbols of data and 132 symbols of redundancy, adding up to a total codeword size of 255 Reed-Solomon symbols.

- **Medium Redundancy:** The intermediate level of redundancy had a code rate of 0.6980, meaning 69.8% of a given packet was used for data. These values resulted in 178 symbols of data and 77 symbols of redundancy in the total of 255 symbols of the codeword,

- **Low Redundancy:** The weakest level of redundancy used allowed for a code rate of 0.8196, meaning a total of 81.96% of a packet could be used for data. This allowed for 209 symbols of data and only 46 of the 255 codeword symbols to be used for redundancy.

The total size of the codeword, namely 255 symbols, was determined by the size of the Galois Field used, in our case a field size of 2^8. This allowed for a max of 2040 bits in each packet to be distributed between data and redundancy. This field size of 2^8 will apply to all symbol-to-bit conversions from now on.

To keep with the desired high redundancy rate, the number of bits in each packet was set at 980 bits. This allowed for minimal padding of 4 bits when using high redundancy levels. In the case of IR-HARQ, all padding was cut before transmission and the packet was reassembled at reception in an attempt to compare it with other schemes.

All schemes were evaluated between 0 dB and 12 dB of E_b/N_0, with 0.5 dB steps between each reading, with the communication channel being modelled by Additive White Gaussian Noise (AWGN). This deliberate selection of SNR values facilitated a comprehensive examination of the system's performance across a wide spectrum of signal strengths, allowing for observing behaviour at both the high and low ends of the SNR spectrum.

By including SNR values at both spectrum extremes, the evaluation captured the convergence of performance metrics as the SNR approached its limits. Furthermore, the utilization of 0.5 dB steps between each SNR measurement ensured an appropriate level of resolution in capturing areas of rapid change in system performance.

4.4.1 ARQ

Packets transmitted using this scheme contain only the 980 bits mentioned above of data and a 32-bit Cyclic Redundancy Check (CRC). All packets transmitted in this way are equal in contents and size.

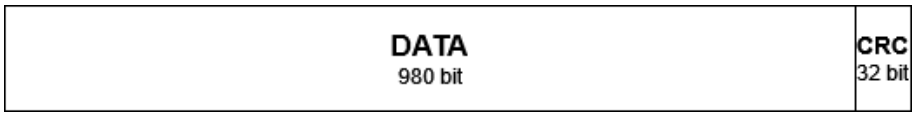

Figure 4.4: Diagram showing the composition of a packet when using the ARQ scheme.

4.4.2 HARQ - Type I

Packets transmitted using Type I HARQ contain 980 bits of data, 4 bits of padding, 1056 bits of redundancy, the equivalent to the High Redundancy level, as well as the 32-bit CRC. This packet is sent every transmission as a whole packet.

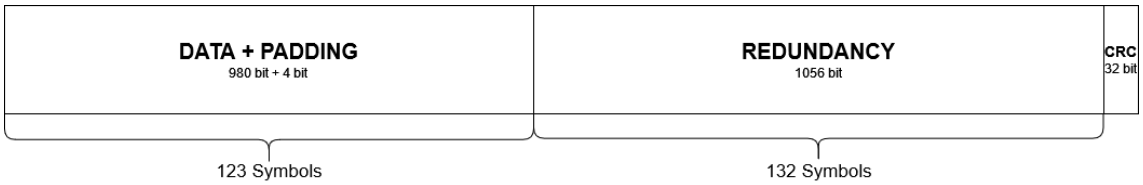

Figure 4.5: Diagram showing the composition of a packet when using the HARQ - Type I scheme.

4.4.3 HARQ - Type II

When using the Type II scheme, data and redundancy are sent alternately. The data packet is sent and contains 980 bits of data, 4 bits of padding, and a 32-bit CRC. The redundancy packet

contains 1056 bits of redundancy as well as a 32-bit CRC. After a data and redundancy packet are sent, another data packet is sent, restarting the cycle.

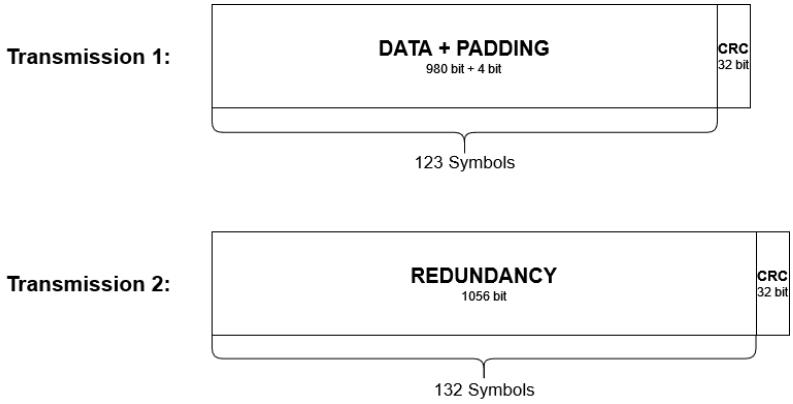

Figure 4.6: Diagram showing the composition of packets when using the HARQ - Type II scheme.

4.4.4 IR-HARQ

When employing the IR-HARQ scheme, there are three distinct packets: the data packet, the weaker redundancy packet and the stronger redundancy packet. These are sent in that order, with the data packet containing 980 bits as well as a 32-bit CRC. The weaker redundancy packet contains either 368 bits of redundancy (Low Redundancy) or 616 bits of redundancy (Medium Redundancy), as well as a 32-bit CRC. The stronger redundancy packet contains either 616 bits of redundancy (Medium Redundancy) or 1056 bits of redundancy (High Redundancy), as well as the 32-bit CRC. The redundancy of the latter packet must always be greater than that of the former.

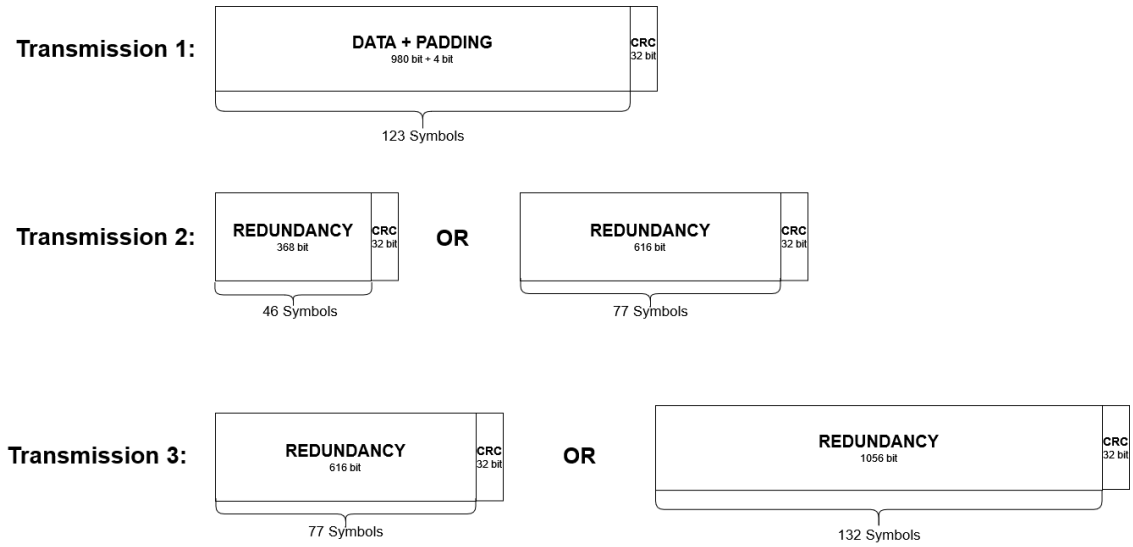

Figure 4.7: Diagram showing the composition of packets when using the IR-HARQ scheme.

Chapter 5

Simulation Results and Analysis

This chapter primarily focuses on the results of our simulation experiments across various scenarios. It includes a detailed analysis of each scenario, comprehensively understanding their individual characteristics and outcomes. Ultimately, the goal is to draw meaningful conclusions that shed light on the performance of the systems and schemes we've examined.

To enhance our comprehension of the results, the tables provided below (5.1 and 5.2) offer a clear summary of both the defined parameters and the scenarios employed in our study. For instance, in table 5.2, different codewords (n,k) mean different levels of protection. (255,123) corresponds to a high level of protection, (255,178) to a medium level and (255,209) to a low level.

Table 5.1: Set of parameters and values used

Energy Levels (E_b/N_0)	From 0 dB to 12 dB, with 0.5 dB steps
Total Data Packets per E_b/N_0	1000 Packets
Data Bits per Packet	980 Bits
FEC Code	Reed-Solomon
Reed-Solomon codes	(255,123) or (255,178) or (255,209)
Modulation	BPSK or QPSK
Maximum Attempts per Packet (M)	3 or 8 transmissions
Channel Type	AWGN or Gilbert-Elliot

Table 5.2: Breakdown of scenarios by (H)ARQ schemes, Reed-Solomon codes (n,k) and simulation variables.

Scenario No.	ARQ	HARQ - Type I (Entire Codeword Tx)	HARQ - Type II (Split Codeword Tx)	IR-HARQ† (Split Codeword Tx)	M	Modulation	Combining	Channel Type
1	X	(255,123)	(255,123)	-	3	BPSK	No	AWGN
2	X	(255,123)	(255,123)	-	8	BPSK	No	AWGN
3	X	(255,123)	(255,123)	(255,123) (255,178)	3 and 8	BPSK	No	AWGN
4	-	-	-	(255,123) (255,178) (255,209)	3 and 8	BPSK	No	AWGN
5	-	-	-	(255,123) (255,178) (255,209)	8	BPSK	Yes	AWGN
6	X	(255,123)	(255,123)	(255,123) (255,178) (255,209)	8	BPSK	II and IR	AWGN
7	-	-	-	(255,123) (255,209)	8	BPSK QPSK	Yes	AWGN
8	X	(127,62)	(127,62)	(127,62) (127,81)	8	BPSK	II and IR	AWGN
9	X	(255,123)	(255,123)	(255,123) (255,209)	8	BPSK	II and IR	AWGN & GE

5.1 First Scenario - (H)ARQ Schemes Comparison with M=3

The first comparison was between the ARQ, HARQ - Type I and HARQ - Type II schemes, with the maximum number of allowed transmissions set at M = 3. The hybrid schemes have a (255,123) code for FEC.

Packet Loss Ratio

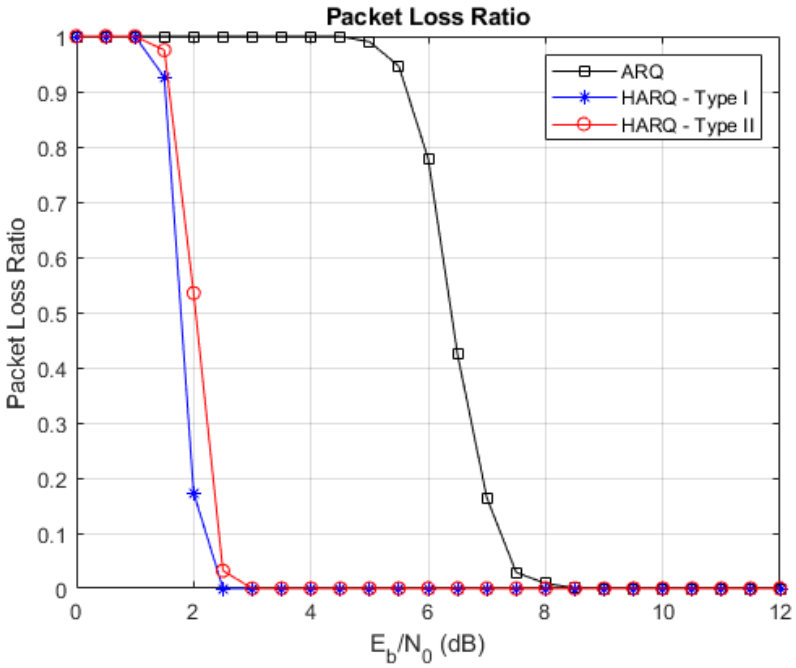

Figure 5.1: Packet Loss Ratio (First Scenario)

As shown in Figure 5.1, ARQ has a much higher range of energy values at which total data loss occurs, with losses only diminishing at 5 dB and above. The other schemes present much closer curves, with a much sharper loss decrease when approaching the 1.5 dB to 2.5 dB range.

Between the two, HARQ - Type I shows a better and quicker improvement due to sending data and redundancy in the same packet, thus having three sets of data and redundancy until total data loss.

HARQ - Type II, on the other hand, needs at least two transmissions to send data and redundancy, thus needing many more transmissions to obtain the same information as Type I. This need for more transmissions and the low value for allowed transmissions explains the higher packet loss when comparing these two schemes.

Average Transmissions per Packet

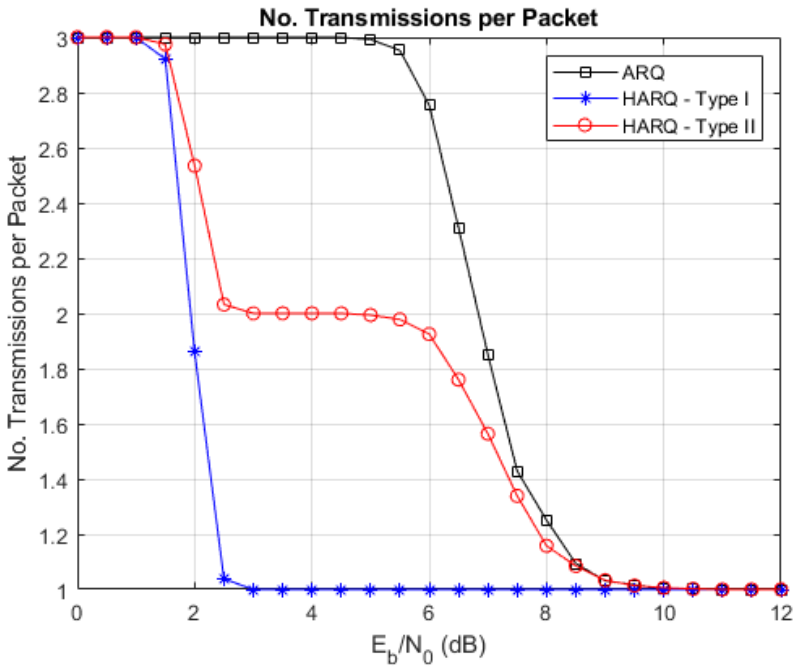

Figure 5.2: Average Transmissions per Packet (First Scenario)

Figure 5.2 shows very different behaviours for the three schemes in analysis.

The curve representing ARQ shows a delayed decline in the number of transmissions as the energy level increases. This delay is associated with the packet loss curve, indicating that a substantial number of packets are needed at very high energy levels to achieve successful transmission.

In contrast to ARQ, HARQ - Type I demonstrates a rapid decline in the number of transmissions with increasing energy levels. This rapid decrease is primarily due to the presence of redundancy in every packet. The redundancy allows for more efficient error correction, resulting in a quicker convergence to successful transmission even at lower energy levels.

HARQ - Type II exhibits a unique pattern in its transmission curve. Initially, there is a reduction in the number of transmissions starting from around 2.5 dB. However, between the energy levels of 3 dB and 5.5 dB, the curve reaches a plateau, indicating that only one data packet and one redundancy packet are required to correct any errors in this range. Beyond 5.5 dB, the curve continues to decline, eventually converging to a single transmission at higher energy levels.

Comparing the three schemes, it is evident that while ARQ and HARQ - Type II both reach a single transmission requirement at approximately 10 dB, HARQ - Type I achieves the same value at a much lower energy level, around 3 dB.

Data Transmission Efficiency

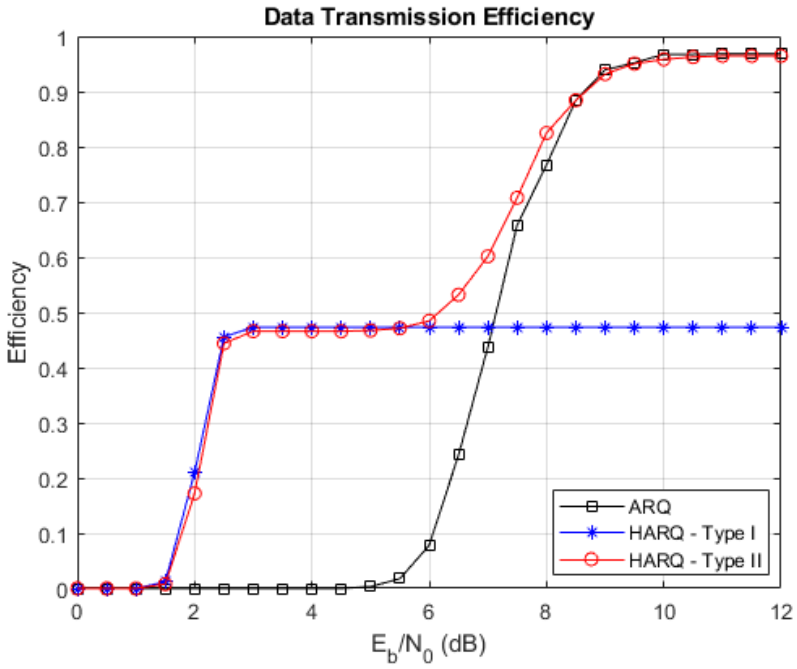

Figure 5.3: Data Transmission Efficiency (First Scenario)

As shown in Figure 5.3, the efficiency of the ARQ scheme is notably low, as indicated by the fact that it only reaches a non-zero value at an energy level of 5 dB. At this point, the scheme slowly starts to improve its efficiency, and it achieves around 50% efficiency at approximately 7 dB. As the energy level continues to increase, the efficiency of ARQ gradually improves, reaching 100% efficiency at 10 dB. However, this improvement process is relatively slow, requiring higher energy levels to achieve optimal efficiency.

HARQ - Type I demonstrates a relatively faster efficiency improvement than ARQ. Its efficiency starts to increase at an energy level of 1.5 dB. This early improvement results from the constant presence of redundancy in every packet, enabling more effective error correction. However, despite this advantage, the redundancy also comes at a cost, as the packet size is approximately double that of a regular data-only packet. Due to this redundancy, the efficiency of HARQ - Type

I plateaus around 50%. It remains at this level as the extra overhead from redundancy counteracts further improvements in efficiency.

The efficiency pattern of HARQ - Type II initially resembles that of HARQ - Type I, showing similar behaviour until an energy level of 6 dB. At this point, a significant improvement occurs in the efficiency of HARQ - Type II. The reason behind this improvement lies in the fact that, at these energy levels, certain packets stop requiring corrections and are transmitted error-free. These lead to a reduction in overhead, positively affecting the overall efficiency of the scheme. As a result, HARQ - Type II's efficiency starts to increase from this point onwards, eventually converging to 100% efficiency. At higher energy levels, the scheme maintains its optimal efficiency as redundancy is less needed.

Normalized Energy

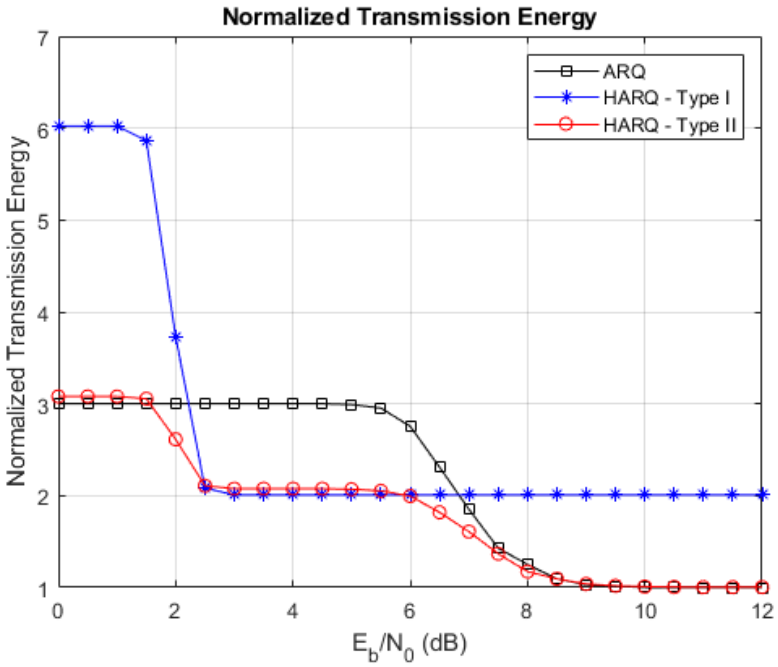

Figure 5.4: Normalized Energy (First Scenario)

In Figure 5.4 the energy consumption of HARQ - Type I is notably higher than the other two schemes from the outset. With its larger packet size, it initially consumes approximately 6 times the reference energy value. This high energy consumption is due to the losses it incurs, necessitating a maximum number of transmissions. As a result, the energy requirements are significantly elevated in the early stages of transmission.

In contrast to HARQ - Type I, both ARQ and HARQ - Type II start with relatively lower energy consumption, approximately half of HARQ - Type I's energy consumption. This similarity in energy consumption is attributed to their comparable packet sizes.

From an energy level of 2 dB onwards, both hybrid schemes, HARQ - Type I and Type II, manage to decrease their energy consumption to approximately 2 times the reference energy value. ARQ stays at 3 times the reference value in this range, indicating that both hybrid schemes are more energy-efficient in comparison, requiring less energy for successful data transmission.

While ARQ and HARQ - Type II continue to decrease their energy consumption, HARQ - Type I experiences stagnation due to its constant packet size. As mentioned before, the larger packet size in HARQ - Type I leads to a constant energy demand despite improvements in the system. However, at an energy level of 5.5 dB, ARQ starts to decrease its energy consumption further, and shortly after, at 6 dB, HARQ - Type II follows suit. Both ARQ and HARQ - Type II converge to the reference energy value, indicating that they achieve optimal energy efficiency at this point.

Scenario Conclusions

The presented metrics offer valuable insights into the performance of the three transmission schemes under specific scenario conditions. From the analysis, it is clear that HARQ - Type I stands out as the most reliable option. It demonstrates superior packet loss performance compared to the other schemes. However, while HARQ - Type II exhibits slightly worse packet loss, its efficiency and energy consumption are significantly better, particularly when channel conditions improve.

5.2 Second Scenario - (H)ARQ Schemes Comparison with M=8

This second comparison maintains all previous characteristics except for the maximum number of transmissions, which has been changed to M = 8.

Packet Loss Ratio

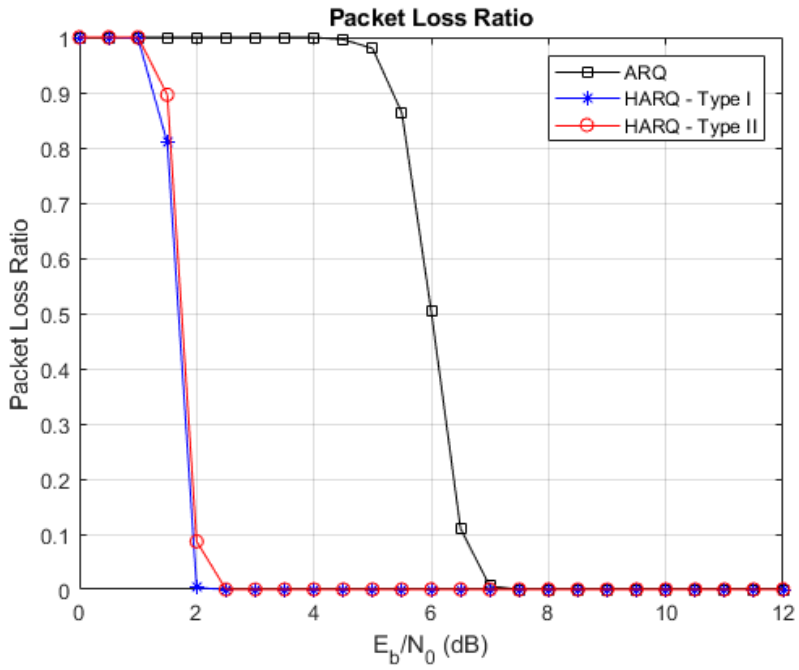

Figure 5.5: Packet Loss Ratio (Second Scenario)

The behaviour of all schemes in this scenario is similar to the one shown in the previous comparison, with slightly less packet loss.

As depicted in Figure 5.5, the total data loss range for ARQ spans a much wider set of energy values, with losses persisting until reaching 4.5 dB and above. On the contrary, the other schemes exhibit closely aligned curves, showcasing a sharper reduction in losses when approaching the energy range of 1.5 dB to 2.5 dB.

Among the two hybrid schemes, HARQ - Type I demonstrates a more efficient and rapid improvement owing to its method of sending data and redundancy in the same packet. This approach results in three sets of data and redundancy being transmitted before encountering total data loss.

In contrast, HARQ - Type II necessitates a minimum of two transmissions to convey both data and redundancy, thus requiring a larger number of transmissions to acquire the same information as Type I. This increased need for transmissions, combined with the limited allowance for transmissions, explains the higher packet loss observed when comparing these two schemes.

Average Transmissions per Packet

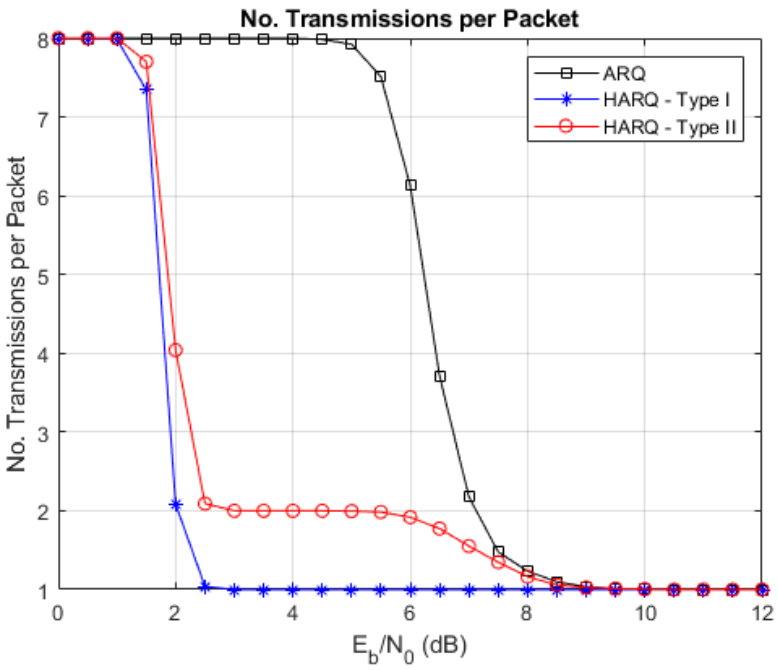

Figure 5.6: Average Transmissions per Packet (Second Scenario)

As shown in Figure 5.6 at lower energy values, all schemes start with the maximum configured number of 8 transmissions. However, the behaviour of the schemes diverges significantly as the energy level increases.

ARQ maintains its maximum transmission count until 5 dB, showing a slower decline in the number of transmissions. As the energy level rises beyond 5 dB, ARQ's transmission count starts decreasing more rapidly, ultimately converging smoothly to one transmission as the channel conditions improve. This gradual reduction in the number of transmissions indicates that ARQ requires higher energy levels to achieve more consistent data delivery.

In contrast, HARQ - Type I exhibits a quicker convergence, reducing its transmission count to one at an energy level of 2.5 dB. This early convergence is attributed to the strategy of including redundancy in every packet, ensuring more effective error correction. As a result, HARQ - Type I efficiently achieves successful data transmission at lower energy levels.

HARQ - Type II demonstrates similar plateaus as in the previous scenario, maintaining a constant transmission count of two, from 2.5 dB to 5.5 dB. This range represents a situation where one redundancy packet consistently suffices to correct errors in the original data, resulting in a steady transmission count. Beyond this range, like ARQ, HARQ - Type II smoothly converges to one transmission as the channel conditions improve, indicating enhanced efficiency as the energy level increases.

Data Transmission Efficiency

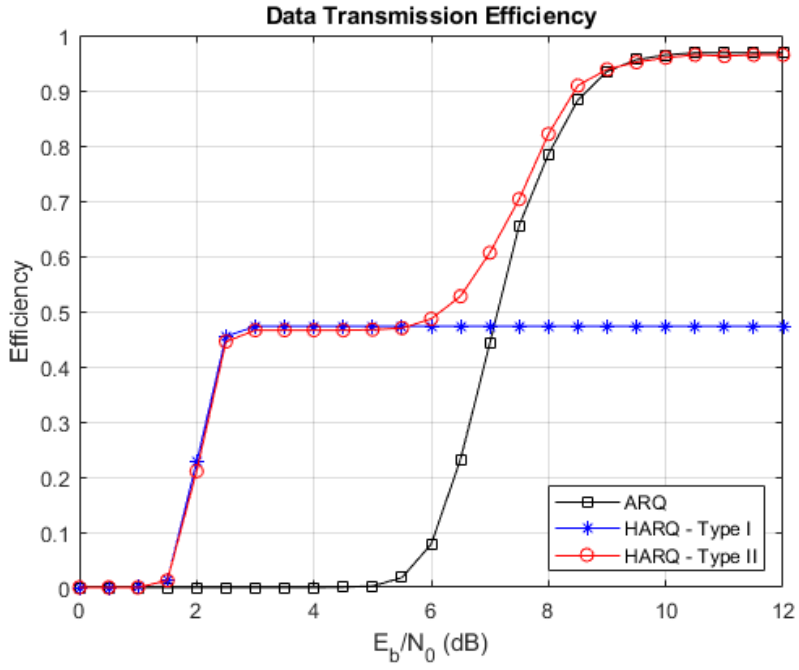

Figure 5.7: Data Transmission Efficiency (Second Scenario)

Figure 5.7 bears a striking resemblance to Figure 5.3, indicating that similar observations can be made, leading to analogous conclusions.

The ARQ scheme demonstrates notably low efficiency, with efficiency becoming non-zero only at an energy level of 5 dB.

HARQ - Type I exhibits a relatively faster efficiency improvement, commencing at an energy level of 1.5 dB. However, it still stagnates at approximately 50% efficiency due to the presence of redundancy at every packet.

Regarding HARQ - Type II, its efficiency pattern initially resembles that of HARQ - Type I, exhibiting similar behaviour until reaching an energy level of 6 dB, at which point its efficiency increases until reaching 100%.

The similarity observed in the efficiency trends across Figure 5.3 and 5.7 suggests that variations in the number of transmissions do not significantly impact the overall efficiency of the transmission schemes. Despite potentially employing a different number of transmissions, the efficiency performance remains relatively stable and comparable.

However, the pivotal point occurs at the threshold where efficiency transitions from zero to a non-zero value. At this critical energy level, both HARQ - Type I and HARQ - Type II display a subtle yet noteworthy enhancement in efficiency. This enhancement is a consequence of both schemes having more data packets and most importantly, redundancies with M = 8, resulting in fewer chances of total data loss.

Normalized Energy

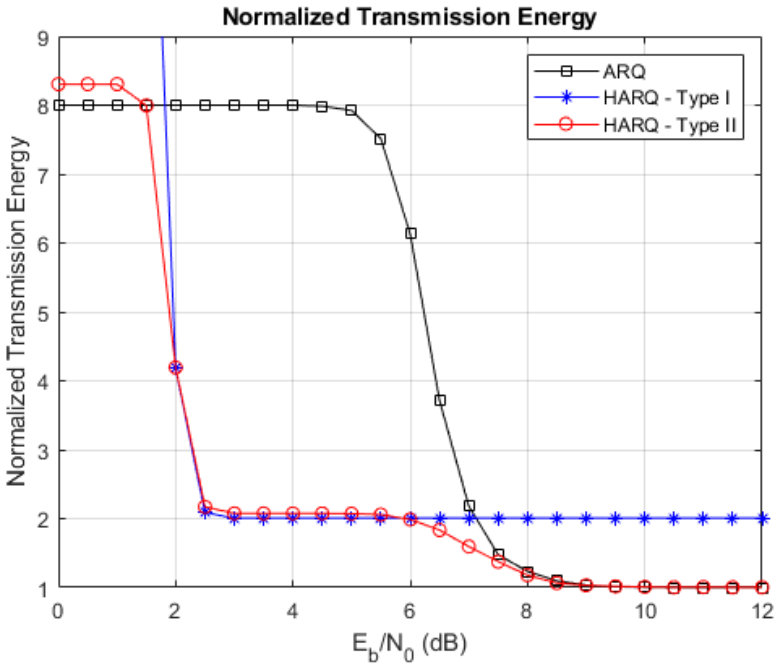

Figure 5.8: Normalized Energy (Second Scenario)

The energy values in Figure 5.8 exhibit a notable difference from the previous observations, primarily due to the increase in the maximum number of transmissions from M = 3 to M = 8. This alteration results in significantly higher initial energy values for the schemes. Specifically, for HARQ - Type I, the energy values start at sixteen times the reference value, while for the other schemes, it is eight times the reference value.

ARQ demonstrates a plateau in energy consumption until the 5.5 dB mark. At this inflexion point, it declines steadily, eventually converging to the reference value.

Both hybrid schemes, HARQ - Type I and HARQ - Type II, exhibit a quick drop in energy consumption from an energy level of 1.5 dB onwards. However, after reaching the 1.5 dB energy level, HARQ - Type I plateaus and maintains a relatively constant energy consumption. In contrast, HARQ - Type II starts to decrease its energy consumption again at 6.5 dB, eventually converging to the reference.

Scenario Conclusions

The same conclusions from the previous scenario can be drawn from this second analysis. HARQ - Type I emerges as the most reliable choice, showcasing superior packet loss performance compared to the other schemes. However, HARQ - Type II, while displaying slightly worse packet loss, excels in efficiency and energy consumption, especially under favourable channel conditions.

Thus, HARQ - Type II proves to be overall a better choice for a wide range of channel conditions.

5.3 Third Scenario - Comparison of (H)ARQ Schemes with IR-HARQ, M=3 and M=8

In this comparison, we introduce the Incremental Redundancy Hybrid Automatic Repeat reQuest (IR-HARQ) scheme as an additional contender alongside existing options. The IR-HARQ scheme incorporates two Forward Error Correction (FEC) codes to enhance its error-correction capabilities. The first FEC code, denoted as (255,178), represents the weakest level of error correction, while the second FEC code, denoted as (255,123), stands as the strongest among the two.

5.3.1 3rd Scenario, M=3

Packet Loss Ratio

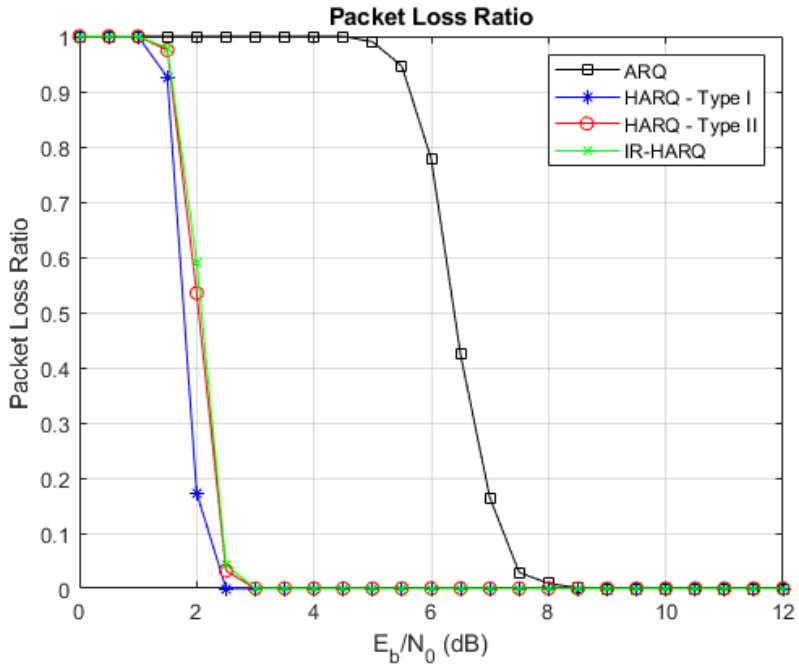

Figure 5.9: Packet Loss Ratio (Third Scenario, M=3)

Figure 5.9 illustrates the behaviour of IR-HARQ compared to the previous schemes. The graph reveals that IR-HARQ exhibits an analogous performance to HARQ Type II, with only a marginal decrease in efficiency. This slight disparity in performance can be attributed to the fact that IR-HARQ necessitates one additional transmission to achieve the same level of redundancy as observed in other hybrid schemes.

Average Transmissions per Packet

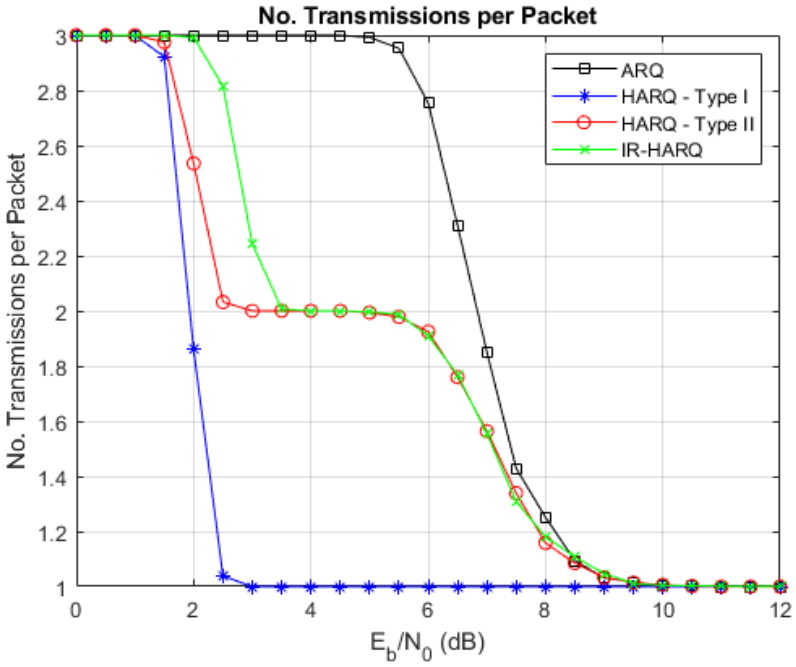

Figure 5.10: Average Transmissions per Packet (Third Scenario, M=3)

In Figure 5.10, when examining the number of transmissions required, it becomes evident that IR-HARQ demands a greater number of transmissions within a specific range, roughly spanning 2 dB to 3.5 dB. This additional transmission is necessary due to the limitations of the first redundancy packet sent, which employs the weaker redundancy of the (255,178) FEC code. Despite its error-correction capabilities, this initial redundancy might be insufficient to entirely correct errors that occurred during the original data transmission. Consequently, a second packet containing additional error correction bits is needed to further address any remaining errors and enhance the chances of successful data recovery.

As the signal-to-noise ratio (SNR) increases and reaches 3.5 dB, the (255,178) FEC code gradually becomes more effective in mitigating errors, to the extent that it can adequately correct any errors resulting from the data transmission. The IR-HARQ scheme plateaus at two transmissions, behaving similarly to HARQ - Type II.

In essence, the behaviour of IR-HARQ in terms of the number of transmissions is shaped by the dynamic interplay between the two FEC codes. Initially, the scheme deploys the weaker (255,178) FEC code, which offers moderate error correction but may require an extra transmission, of the (255,123) code, to ensure complete error recovery. As the SNR improves, the (255,178) code becomes more adequate and can manage errors with just two transmissions, paralleling the behaviour of HARQ - Type II.

Data Transmission Efficiency

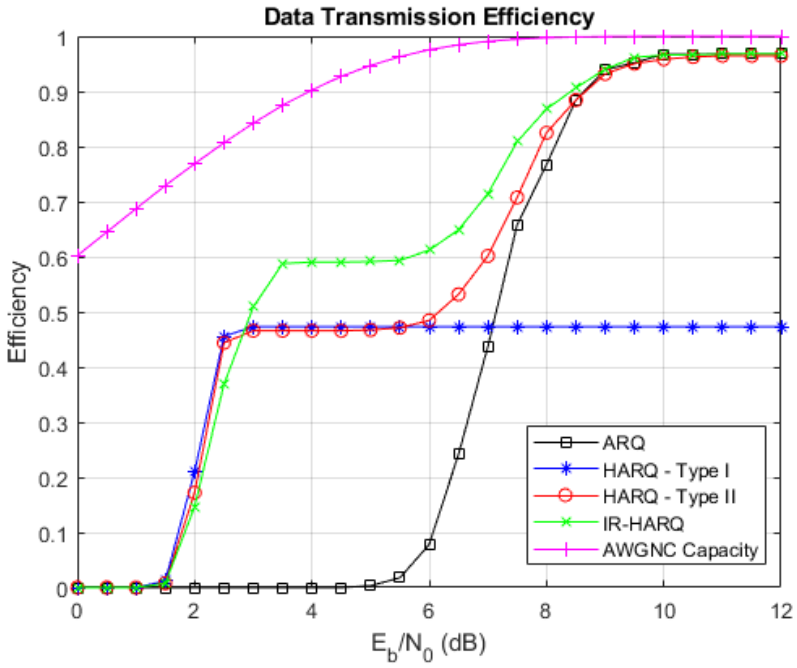

Figure 5.11: Data Transmission Efficiency (Third Scenario, M=3)

As seen in Figure 5.11 the primary strength of IR-HARQ lies in its remarkable Transmission Efficiency, setting it apart from the other two hybrid schemes. While its initial performance increase might show only a marginal improvement, almost on par with the other schemes or slightly worse, this changes rapidly due to its unique capability of sending a more minor redundancy when it can effectively correct all errors. This adaptive feature sets IR-HARQ on a trajectory of substantial progress, allowing it to surpass the other schemes quickly.

The breakthrough in efficiency becomes evident, with a significant improvement of nearly 10%, particularly noticeable within the SNR range of 3.5 dB to 5.5 dB. This range is precisely where the (255,178) FEC code proves to be adequately effective but not overly redundant.

This remarkable performance superiority continues until IR-HARQ reaches its convergence point at an efficiency of 100%.

Normalized Energy

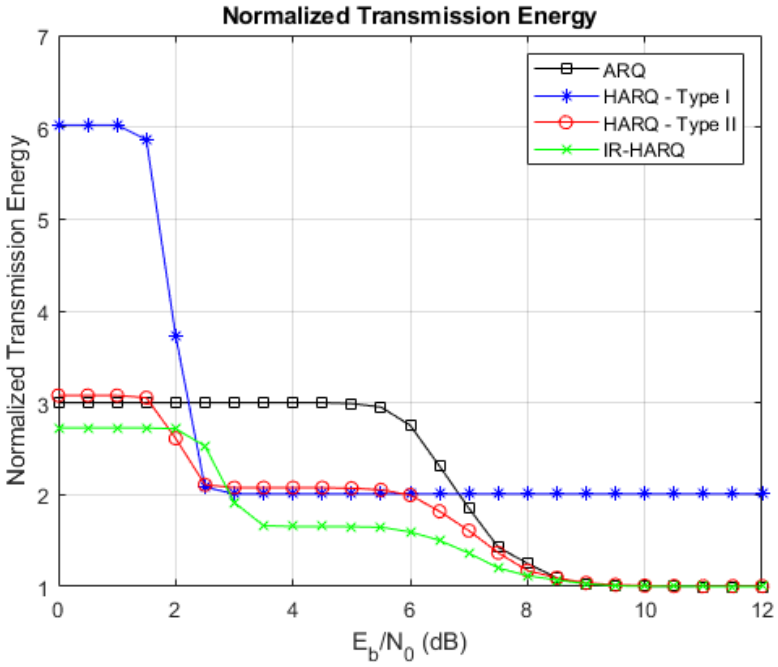

Figure 5.12: Normalized Energy (Third Scenario, M=3)

In Figure 5.12 IR-HARQ again shows some improvement. Due to the smaller size of its second packet, it consumes less energy in the region with total data loss. Following this is a region with slightly worse performance in the 2 dB to 2.5 dB range, where its efficiency was also barely worse than the other hybrid schemes.

This region, however, is followed by one of decline in energy consumption comparatively to the other schemes. Hence, during the 3.5 dB to 5.5 dB range, it consumes approximately 1.65 times the reference value, while its closer comparison, HARQ - Type I uses over 2 times the reference value.

5.3.2 3rd Scenario, M = 8

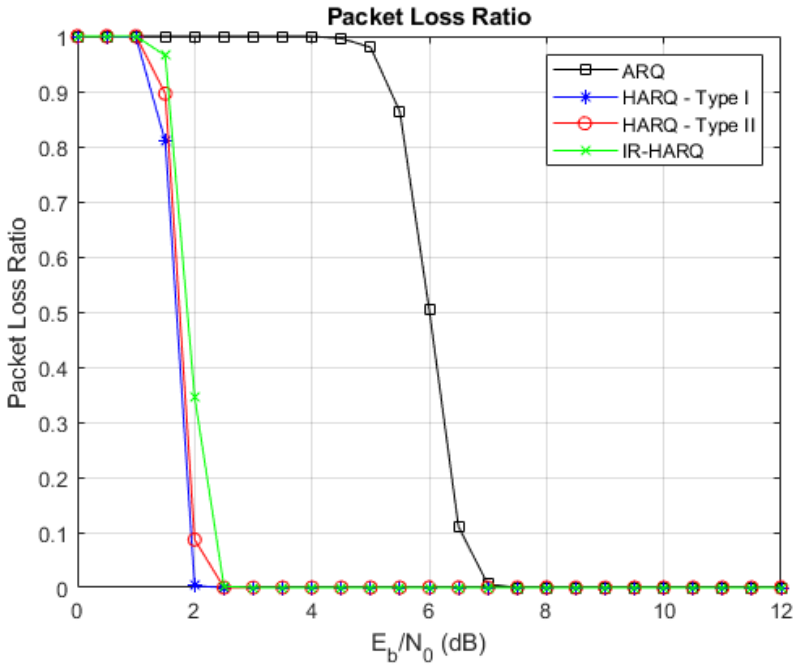

Figure 5.13: Packet Loss Ratio (Third Scenario, M=8)

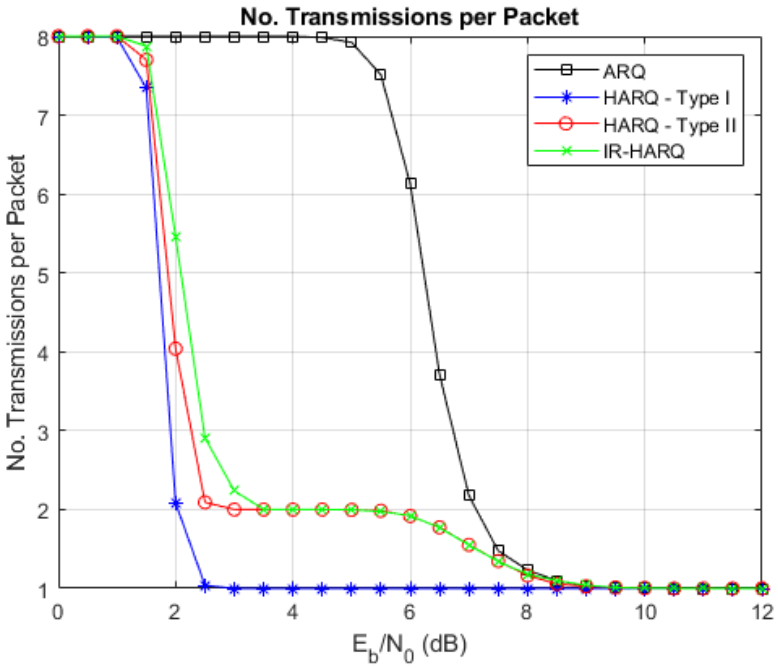

Figure 5.14: Average Transmissions per Packet (Third Scenario, M=8)

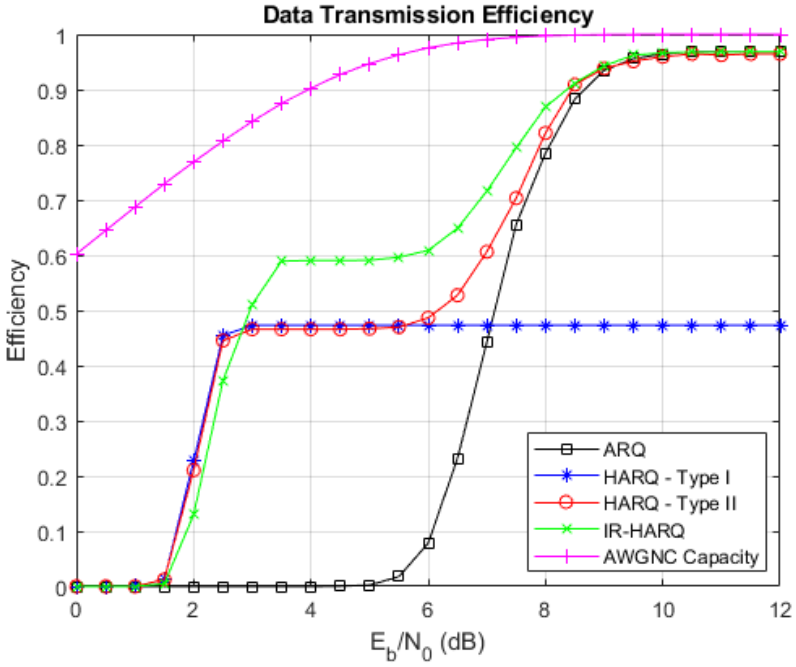

Figure 5.15: Data Transmission Efficiency (Third Scenario, M=8)

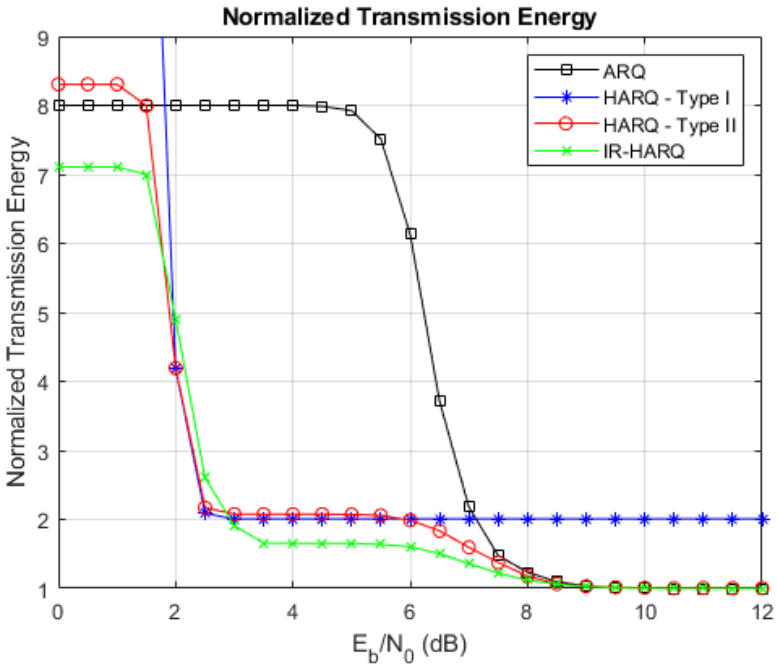

Figure 5.16: Normalized Energy (Third Scenario, M=8)

Aside from a worse performance in packet loss in the 1.5 dB to 2 dB range as can be seen in Figure 5.13 when compared to Figure 5.9, IR-HARQ presents the same or a nearly identical behaviour in all metrics, and, as such, the same observations can be made. While offscreen, the starting energy value for HARQ - Type I is sixteen times the reference.

Scenario Conclusions

Considering all aspects, IR-HARQ emerges as a superior and more efficient alternative to HARQ - Type II. While it is true that IR-HARQ may encounter slightly more packet loss in certain situations, this drawback is limited to a very small range of energy values. In contrast, the advantages of better efficiency and energy consumption are prevalent across a broader spectrum of channel conditions.

The slight increase in packet loss in IR-HARQ is primarily offset by its exceptional efficiency in adapting its redundancy and error-correction capabilities.

5.4 Fourth Scenario - Comparison of IR-HARQ variants

This comparison scenario focuses on three versions of the IR-HARQ scheme with different (n,k) pairs: the previously used with (255,178) and (255,123) codes, and two new ones, (255,209) as the weaker and (255,123) as the stronger, as well as, (255,209) as the weaker and (255,178) as the stronger.

5.4.1 Fourth Scenario, M = 3

Packet Loss Ratio

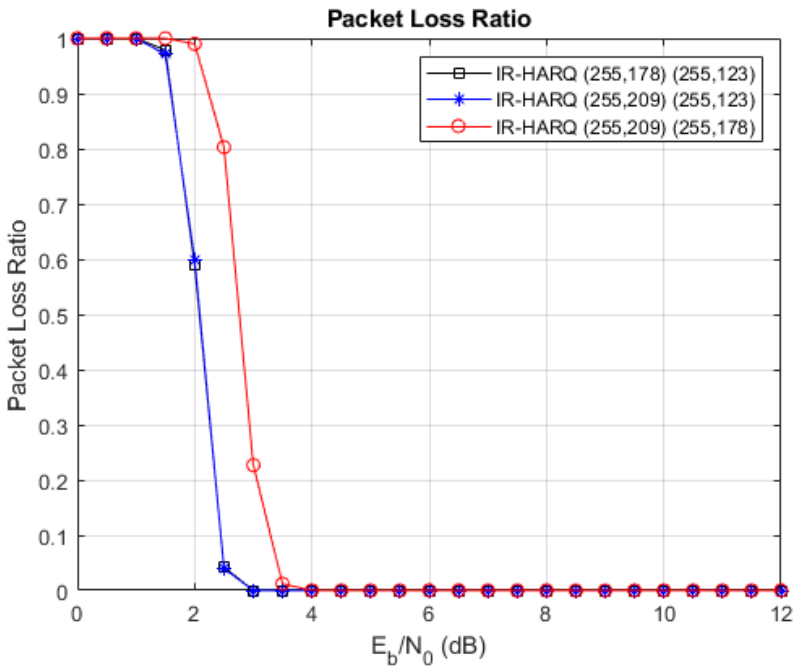

Figure 5.17: Packet Loss Ratio (Fourth Scenario, M=3)

In Figure 5.17, the packet loss graph reveals interesting insights into the performance of different schemes employing varying FEC codes. Specifically, the two schemes employing the stronger redundancy of (255,123) exhibit noticeable improvements in packet loss at an earlier stage and with a similar rate of improvement. On the other hand, the scheme utilizing the (255,178) FEC code faces limitations in its error-correction capabilities, resulting in poorer packet loss performance overall.

Average Transmissions per Packet

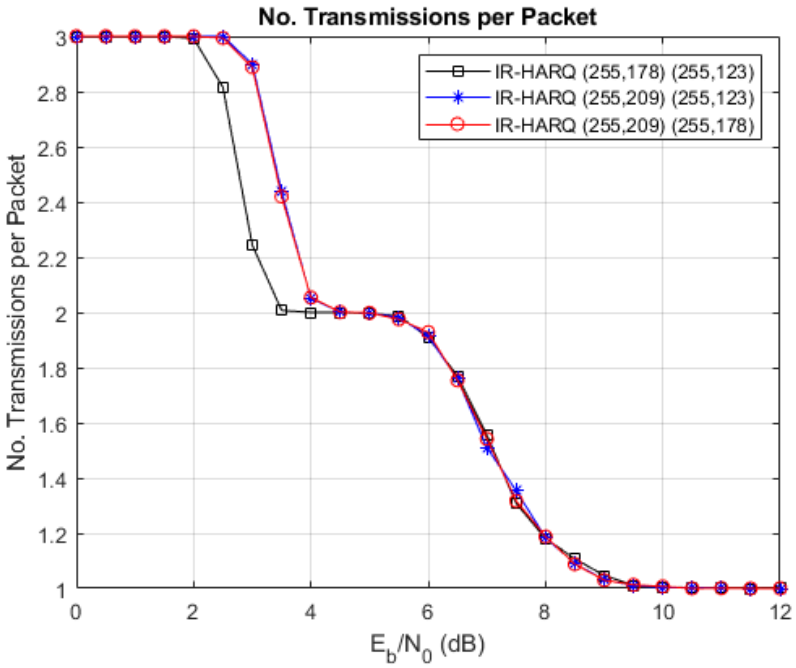

Figure 5.18: Average Transmissions per Packet (Fourth Scenario, M=3)

As Figure 5.18 depicts, in terms of transmissions, a noticeable distinction arises between the two schemes that utilize FEC codes with lower error correction capabilities in their first packets. Specifically, the schemes employing the weaker FEC code of (255,209) exhibit more transmissions per packet than those with the slightly stronger (255,178) FEC code. The underlying reason for this difference lies in the varying error correction capabilities of the two FEC codes.

The (255,209) FEC code proves less adept at error correction than the (255,178) code. Consequently, when errors occur during data transmission, the (255,209) code faces limitations in effectively correcting these errors within a single transmission. As a result, it requires additional retransmissions of stronger codes.

Data Transmission Efficiency

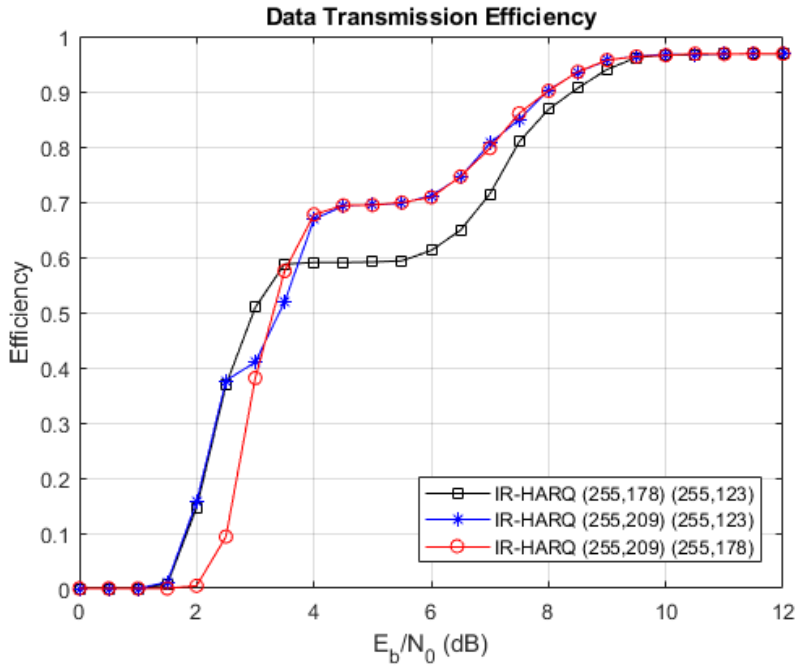

Figure 5.19: Data Transmission Efficiency (Fourth Scenario, M=3)

Figure 5.19 displays three different behaviour patterns, each corresponding to a specific scheme. The graph illustrates the efficiency of different IR-HARQ schemes with varying code strengths.

As shown, the schemes using (255.123) exhibit an early efficiency improvement compared to those using the (255,178) code. This is primarily due to the superior error correction capabilities of the stronger code, allowing for more effective error recovery after data transmission.

However, after a certain point, the behaviour shifts when we examine the IR-HARQ schemes employing a weaker redundancy of (255,209). Surprisingly, these schemes overtake the one with a weaker redundancy of (255,178) in efficiency by nearly 10%. All schemes then plateau before beginning to rise and converging to 100%.

Interestingly, the scheme with the weakest, weaker redundancy, and strongest stronger redundancy exhibits the best behaviour of all three schemes, with the early rise of the strongest redundancy and the higher plateau of the weaker redundancy. This scheme is only less efficient in a small region, around 3.5 dB.

Normalized Energy

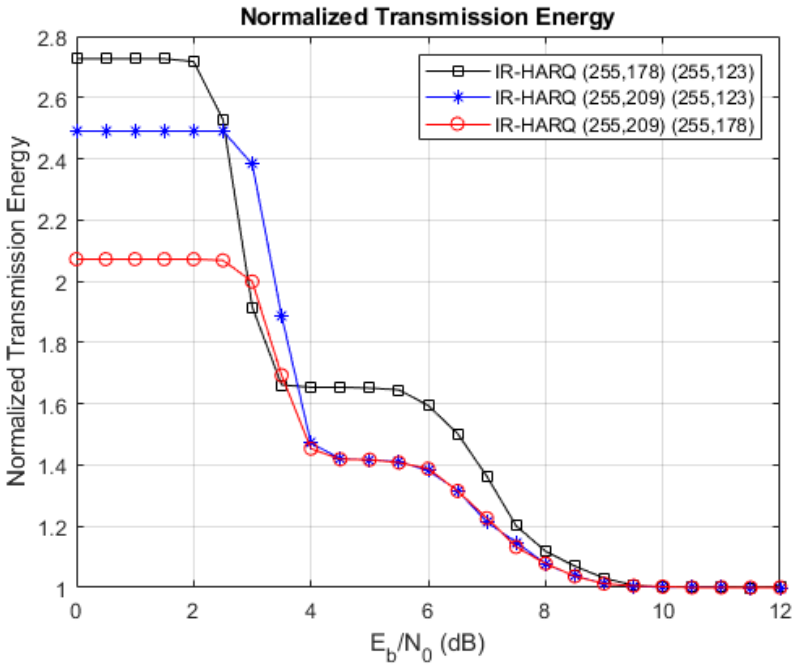

Figure 5.20: Normalized Energy (Fourth Scenario, M=3)

As seen in Figure 5.20 initially, the graph demonstrates noticeable differences among the schemes, and this variance arises from their unique set of bit sizes per packet. Among these schemes, IR-HARQ (255,209) (255,178) exhibits the most favourable results in terms of energy consumption. This outcome is particularly evident in the region of total data loss, where these schemes shine compared to the others.

However, it is essential to note that this advantage applies solely to the region of total data loss. When comparing the schemes outside this specific region, both schemes with a weaker redundancy of (255,209) display a notable decrease in energy consumption when contrasted with the other scheme, which utilizes the (255,178) redundancy.

Quantitatively, the energy consumption of the (255,209) schemes is approximately 0.2 reference values lower in the range of 4 dB to 5.5 dB when compared to the scheme with a weaker redundancy of (255,178).

As we move beyond this range, the improvement in energy consumption gradually diminishes. This is because, at this point, all schemes approach the reference value regarding energy efficiency.

5.4.2 Fourth Scenario - M = 8

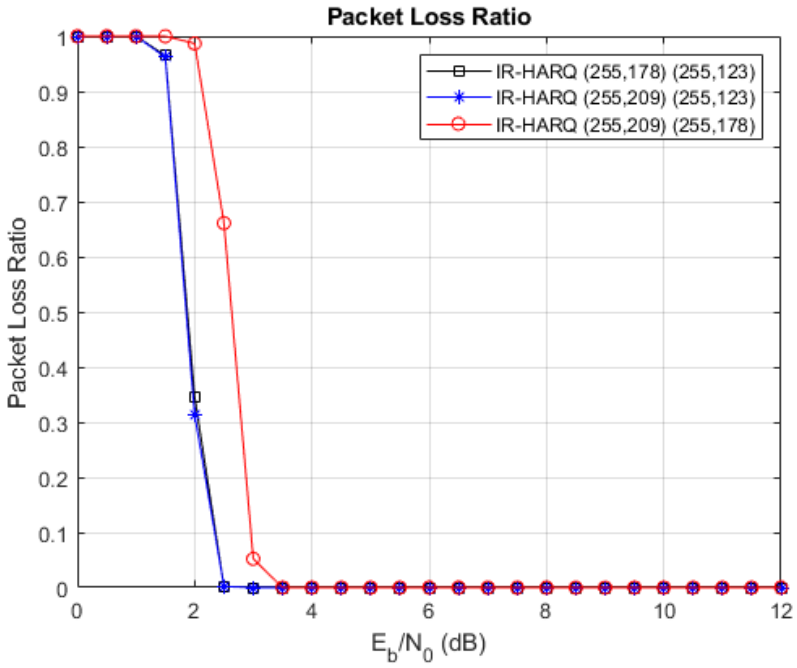

Figure 5.21: Packet Loss Ratio (Fourth Scenario, M=8)

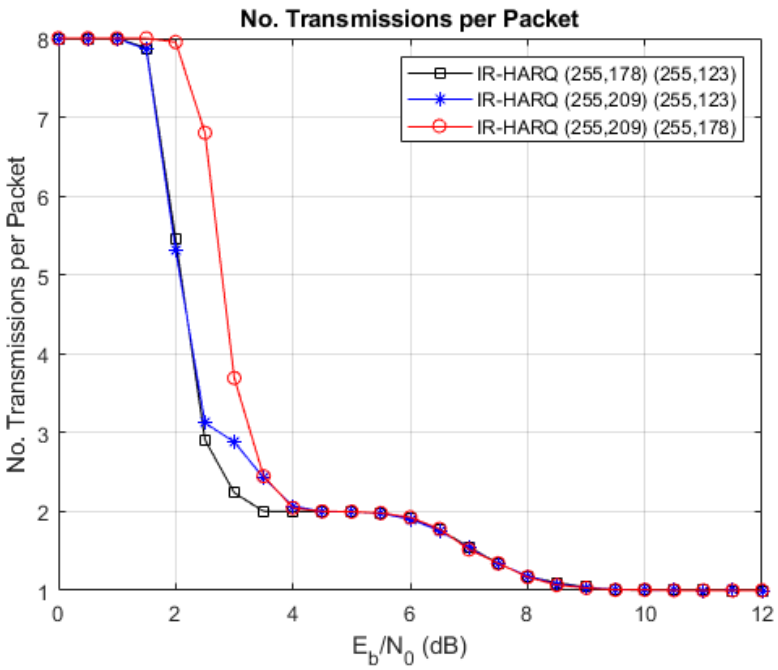

Figure 5.22: Average Transmissions per Packet (Fourth Scenario, M=8)

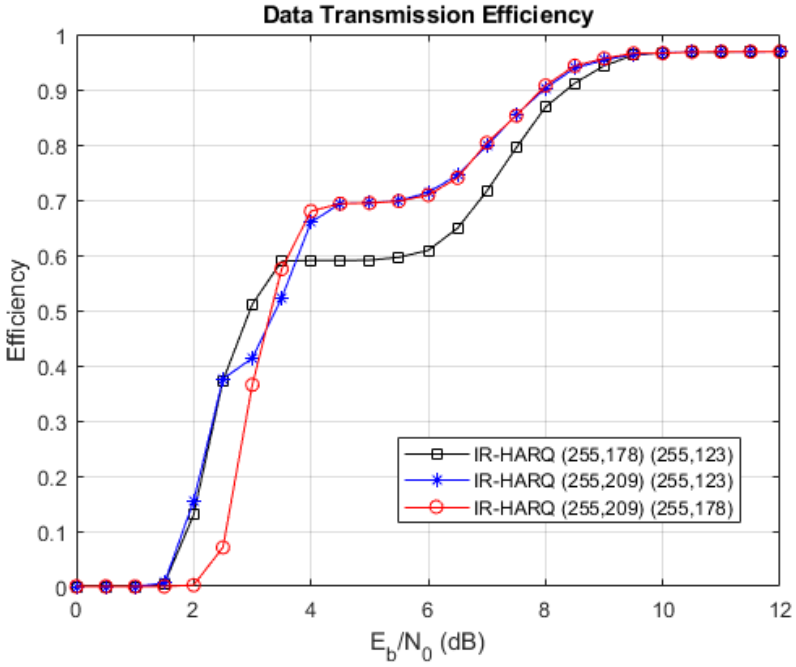

Figure 5.23: Data Transmission Efficiency (Fourth Scenario, M=8)

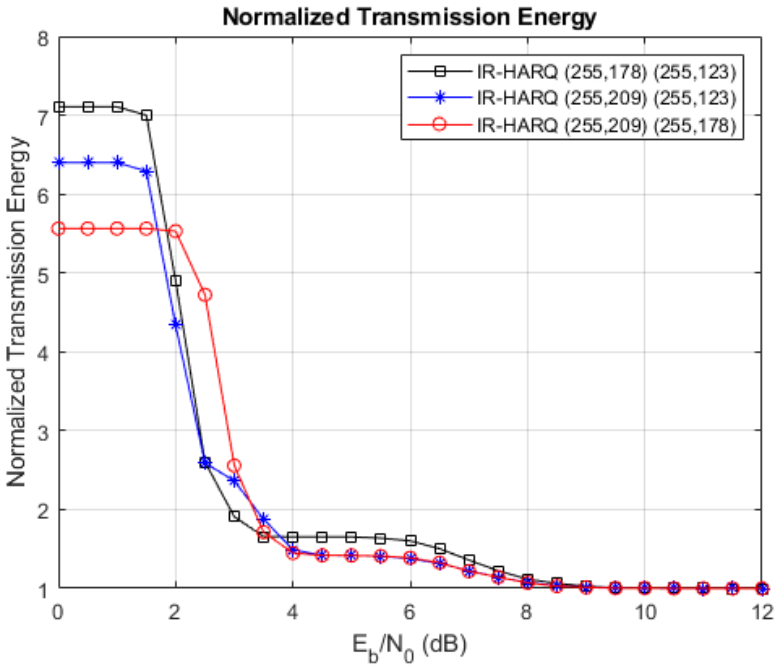

Figure 5.24: Normalized Energy (Fourth Scenario, M=8)

The findings and conclusions drawn in 5.4.1 are reaffirmed and further supported by the data depicted in Figures 5.21, 5.22, 5.23, and 5.24. The same behaviours can be observed, with only slight improvements in the critical region of 2 dB to 3.5 dB and initial higher energy consumption, both due to the increase of the maximum number of transmissions from three to eight.

Scenario Conclusions

After thoroughly analysing all three variants of the IR-HARQ scheme, it becomes evident that IR-HARQ (255,209) (255,123) stands out as the top-performing scheme among them. This variant combines the weakest weak code of (255,209) with the strongest (255,123) code, resulting in remarkable adaptability and superior performance over the other two tested schemes in a large spectrum of energy levels.

The key strengths of IR-HARQ (255,209) (255,123) lie in its unique combination of characteristics. Firstly, it benefits from the fast improvements in efficiency associated with the strong (255,123) code after the region of total data loss. Furthermore, the weaker (255,209) code exhibits equal or higher efficiency at medium-range energy levels than other schemes.

The only region where IR-HARQ (255,209) (255,123) lags behind is 3.5 dB. However, it is noteworthy that this region appears most suitable for the (255,178) code, indicating that each variant has its own strengths in specific conditions.

Overall, IR-HARQ (255,209) (255,123) possesses the best characteristics of the other two schemes and demonstrates the most optimal performance across various scenarios.

5.5 Fifth Scenario - Comparison of IR-HARQ with Code-Combining

In this comparison, our focus shifts towards the implementation of code-combining techniques in two of the IR-HARQ schemes that were previously examined. We will analyse the performance of these schemes with and without the application of code combining.

Packet Loss Ratio

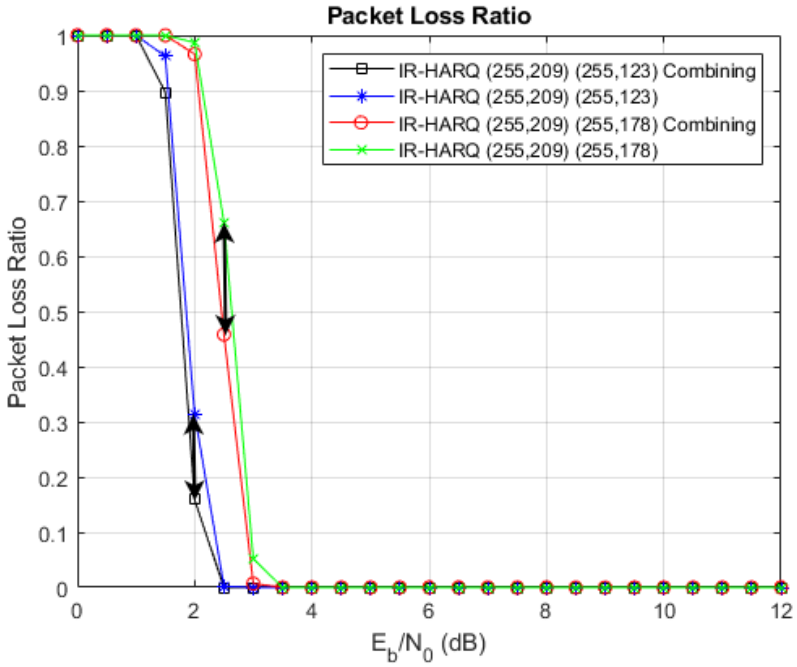

Figure 5.25: Packet Loss Ratio (Fifth Scenario)

Figure 5.25 clearly shows the effects combining has on both IR-HARQ variants.

The graph demonstrates that IR-HARQ (255,209) (255,178) experiences a noticeable improvement in performance within the critical range of 1.5 dB to 3.5 dB SNR. The initial packet loss rate without code combining is around 65%. However, after applying code combining, this rate is reduced to approximately 45% within the critical SNR range. The right arrow further emphasizes this difference. While the improvement is evident, the resulting 45% packet loss is still considered relatively high for many practical applications, making this variant less desirable in scenarios where more reliable and robust transmission is required.

In contrast, the results for IR-HARQ (255,209) (255,123) reveal more promising outcomes with the utilization of code combining. The initial packet loss rate without code combining is over 30% at certain SNR levels. However, with the implementation of code combining, this rate is significantly reduced to approximately 15% within the critical SNR range. This substantial decrease in packet loss results in a much more manageable error rate, making this variant more suitable for applications that demand higher reliability and lower packet loss. This difference is made more evident by the left arrow.

The findings from IR-HARQ (255,209) (255,123) underscore the potential benefits of code combining. By leveraging this technique, the variant achieves significant performance gains, particularly in scenarios with moderate to low SNR values.

Average Transmissions per Packet

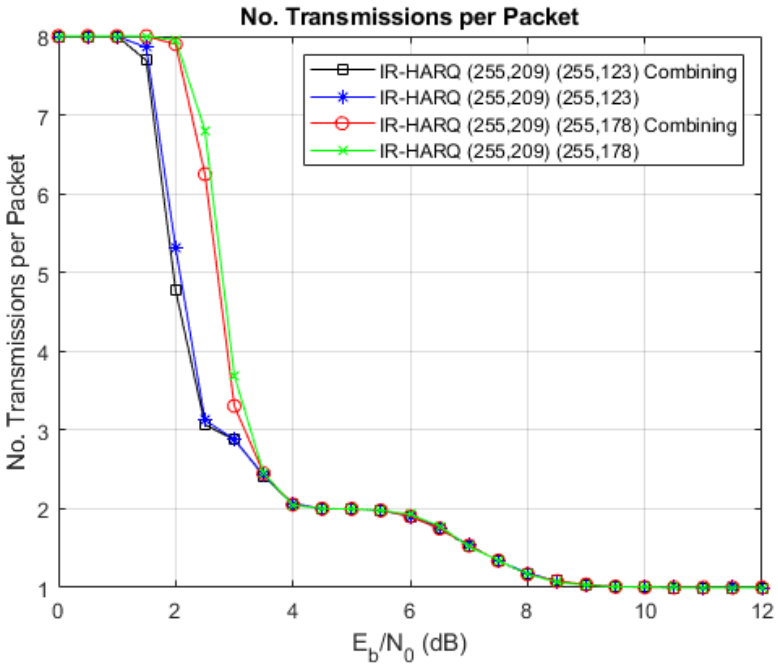

Figure 5.26: Average Transmissions per Packet (Fifth Scenario)

The observed effects of code combining, as depicted in Figure 5.25, are similarly evident in Figure 5.26. Both figures demonstrate a noticeable impact on performance. Particularly in the critical range, where the curves exhibit a steep decline, the utilization of code combining significantly reduces the average number of transmissions by up to 0.5 transmissions per packet.

The observed improvement in transmission efficiency can be attributed to the fundamental behaviour exhibited when employing code combining techniques. When code combining is utilized, all received data packets are systematically combined with every redundancy packet available, encompassing a comprehensive exploration of all possible combinations. This exhaustive approach allows the system to make the most out of the redundancy information at its disposal.

In contrast, the scenario without code combining only pairs each data packet with the subsequent redundancy packet it encounters. Consequently, this limited pairing approach fails to explore the full potential of redundancy utilization, as it solely relies on adjacent packets for error correction.

Data Transmission Efficiency

As can be seen in Figure 5.27 analysing the efficiency of all schemes reinforces the benefits of code-combining. The combining variants show a slight improvement over their non-combining counterparts in the lower ranges of energy values. After reaching the plateau, all behave similarly and converge to near 100%.

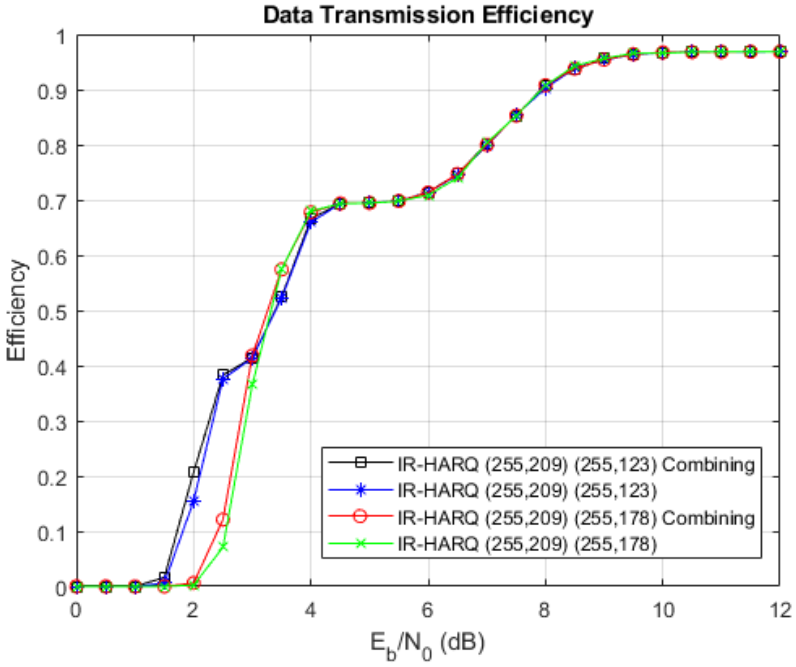

Figure 5.27: Data Transmission Efficiency (Fifth Scenario)

Normalized Energy

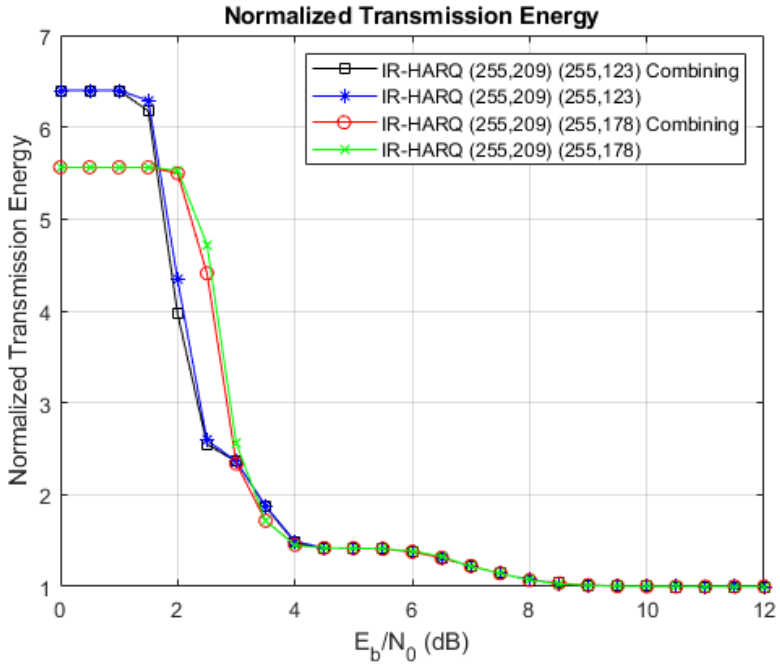

Figure 5.28: Normalized Energy (Fifth Scenario)

Figure 5.28 shows that an in-depth analysis of energy consumption further solidifies the previously observed trends, providing compelling evidence in favour of code combining as a superior

approach. Throughout the entire spectrum of energy values, it becomes evident that all schemes utilizing code combining consistently outperform, or at the very least, match the performance of their non-combining counterparts.

Scenario Conclusions

Following a meticulous and comprehensive analysis of each metric, a compelling conclusion emerges: the adoption of code combining presents substantial benefits that more than justify the increase in implementation complexity.

Across all evaluated metrics, code combining consistently demonstrates superior performance compared to previously employed schemes, with packet loss being one of the most notable areas of improvement. Furthermore, when integrated with the already effective IR-HARQ (255,209) (255,123) technique, code combining further elevates the overall performance to new heights.

5.6 Sixth Scenario - Single and Dual Node Energy Analysis

This sixth comparison focuses solely on the energy consumption metric. Namely, while all other energy graphs were obtained considering only the energy perspective of a single node, as seen in Figure 4.2, this scenario takes into consideration the energy consumption of the other node. One thing to remark is that, when analysing from the perspective of both nodes, the reference value also changes accordingly.

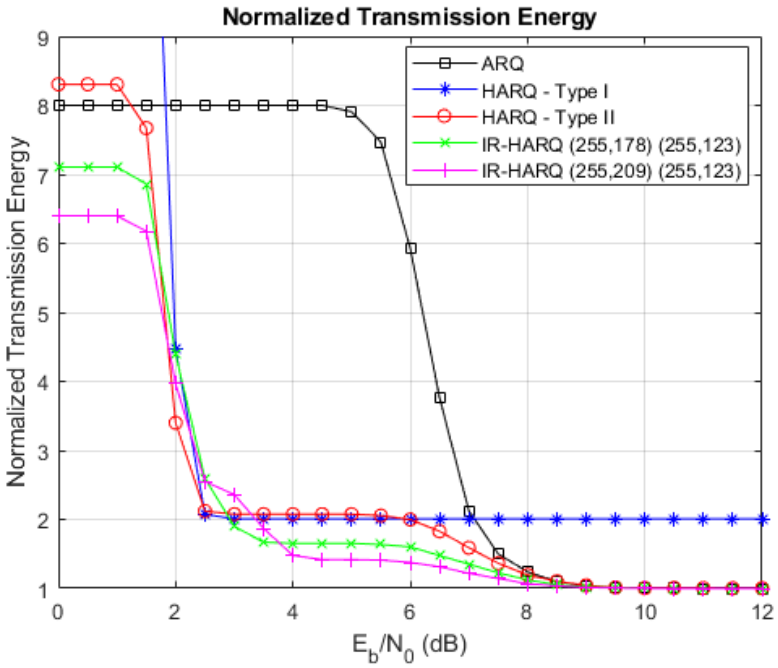

Figure 5.29: Normalized Energy from the perspective of a single node. (Sixth Scenario)

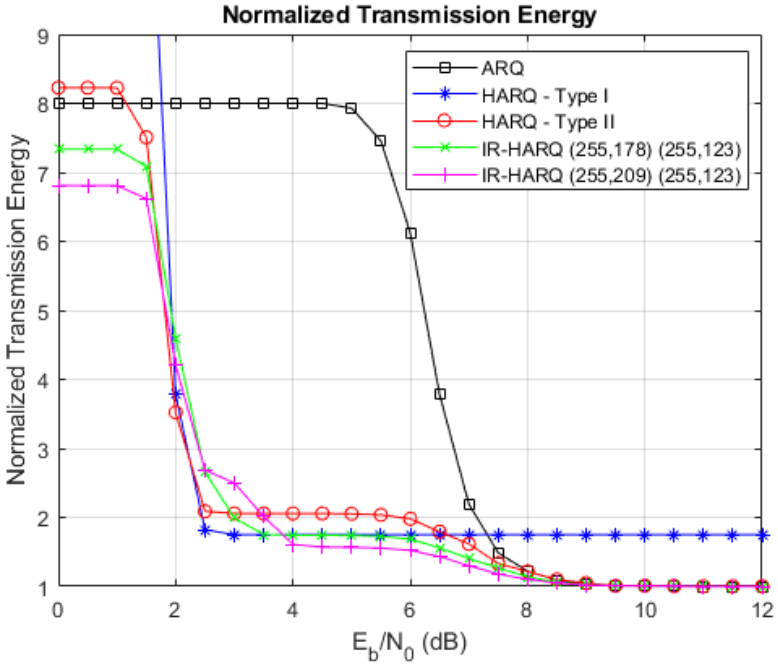

Figure 5.30: Normalized Energy from the perspective of both nodes. (Sixth Scenario)

For Figure 5.29 the starting energy value for HARQ - Type I is 16 times the reference, while in Figure 5.30 it is closer to 14 times. The analysis of both graphs, in Figures 5.29 and 5.30 provides valuable insights that extend beyond the single node perspective, demonstrating that the conclusions drawn from individual nodes also hold true when considering both nodes in the communication system. This observation reinforces the significant energy savings that can be achieved by employing IR-HARQ schemes. The benefits of these schemes apply not only to the transmitter but also to the receiver, resulting in decreased energy consumption for the entire system.

Scenario Conclusions

In conclusion, analysing both nodes in the communication system reaffirms the advantages of implementing IR-HARQ schemes. The energy savings and efficiency gains observed in the single node perspective apply consistently when considering both the transmitter and receiver. This comprehensive energy optimization showcases the practicality and value of IR-HARQ in enhancing overall energy efficiency.

5.7 Seventh Scenario - Comparison between BPSK and QPSK

In this comparison, we focus on the overall best-performing scheme from the previous analyses, which is the IR-HARQ (255,209) (255,123) technique. We now explore its performance with two distinct modulation schemes: Binary Phase Shift Keying (BPSK) and Quadrature Phase Shift Keying (QPSK).

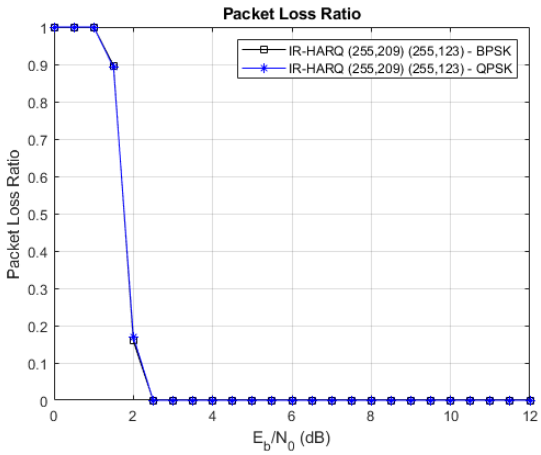

(a) Packet Loss Ratio

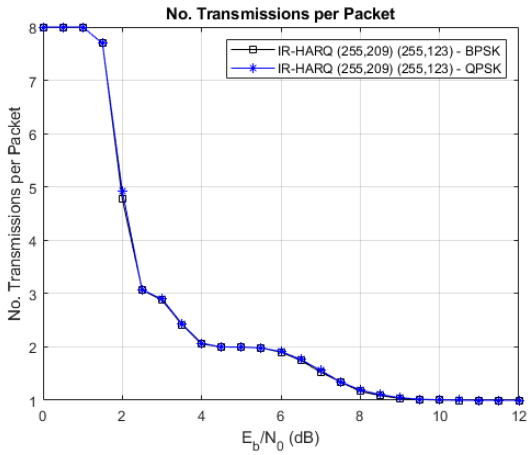

(b) Average Transmissions per Packet

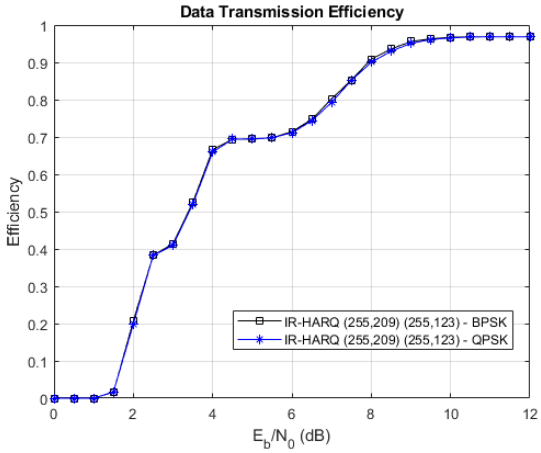

(c) Data Transmission Efficiency

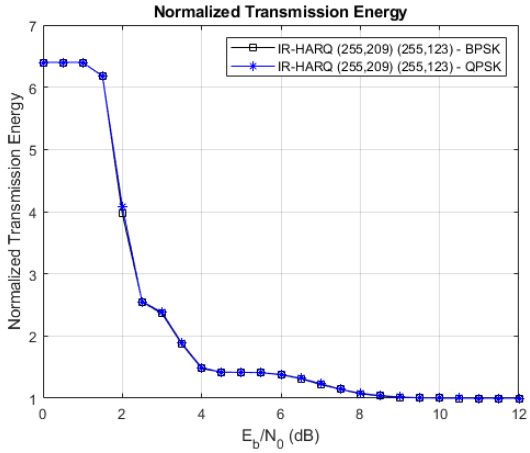

(d) Normalized Energy

Figure 5.31: Diagram Representations of all Metrics (Seventh Scenario)

The comprehensive analysis of Figures 5.31a, 5.31b, 5.31c, and 5.31d reveals a noteworthy observation: the behaviour and values of the performance metrics remain highly similar when utilizing both modulations, BPSK and QPSK.

Scenario Conclusions

Upon conducting a comprehensive analysis of both modulations, BPSK and QPSK, it becomes evident that their effectiveness is remarkably similar across all evaluated metrics. Both modulations demonstrate commendable performance in packet loss, throughput, energy efficiency, and energy consumption, with only minor variations observed at specific points.

However, despite the close similarity in performance, a key differentiating factor emerges: the data throughput. QPSK offers a distinct advantage, providing higher data throughput than BPSK. This advantage stems from the ability of QPSK to convey two bits of data per symbol, as opposed to BPSK's one bit. The increased data throughput of QPSK makes it particularly well-suited for scenarios that require higher data rates and more efficient utilization of available bandwidth.

As a result, considering the higher data throughput offered by QPSK, it emerges as the most suitable option in many practical applications. In scenarios where maximizing data transmission speed is a priority, QPSK presents an advantageous choice, ensuring faster data delivery and enhanced overall communication performance.

Furthermore, the selection of QPSK does not compromise on other aspects of performance. As observed in the analysis, QPSK still maintains impressive packet loss, energy efficiency, and energy consumption performance, remaining on par with BPSK in these metrics.

5.8 Eight Scenario - Reduction in Packet Size

In this scenario, we compare the performance and metrics across all schemes when the packet size is reduced to 496 bits. The size of the maximum redundancy is also reduced to 66 Reed-Solomon symbols, or 528 bits. This version of IR-HARQ also includes a weaker redundancy of 46 symbols.

The primary objective of this comparison is to determine whether the benefits and advantages previously observed in the context of IR-HARQ still hold when dealing with smaller packet sizes.

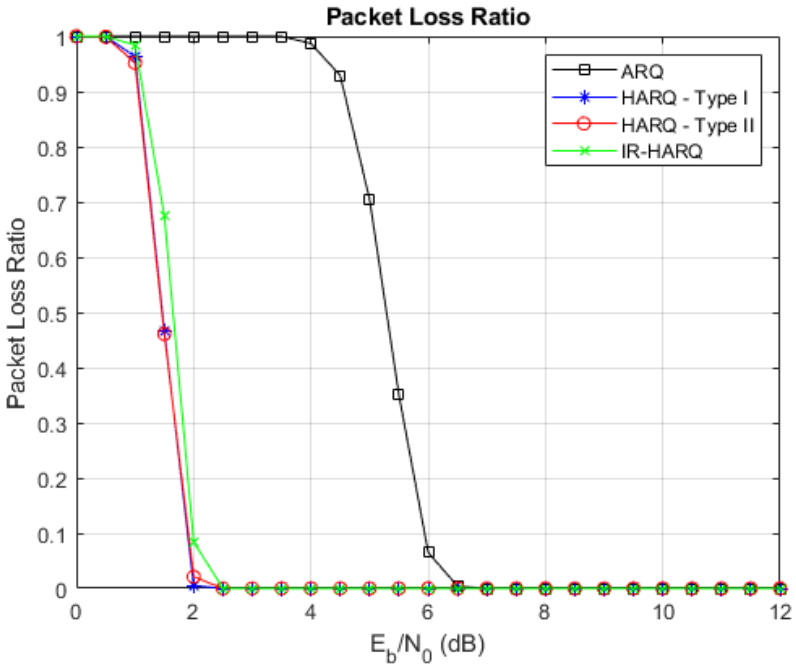

Figure 5.32: Packet Loss Ratio (Eight Scenario)

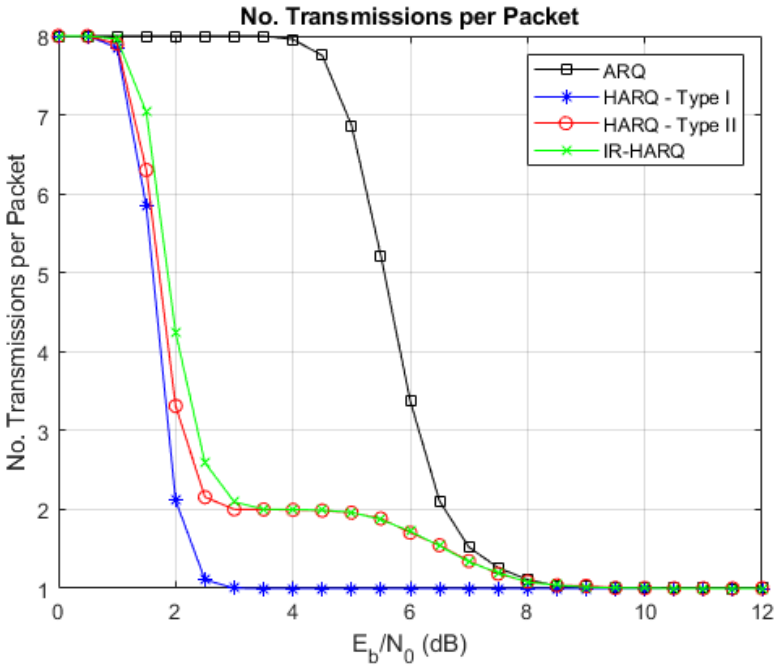

Figure 5.33: Average Transmissions per Packet (Eight Scenario)

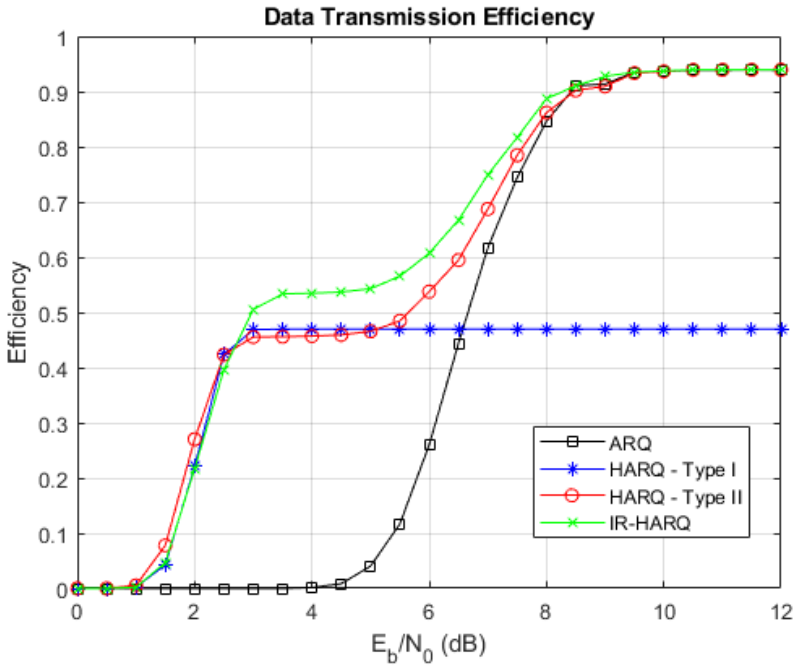

Figure 5.34: Data Transmission Efficiency (Eight Scenario)

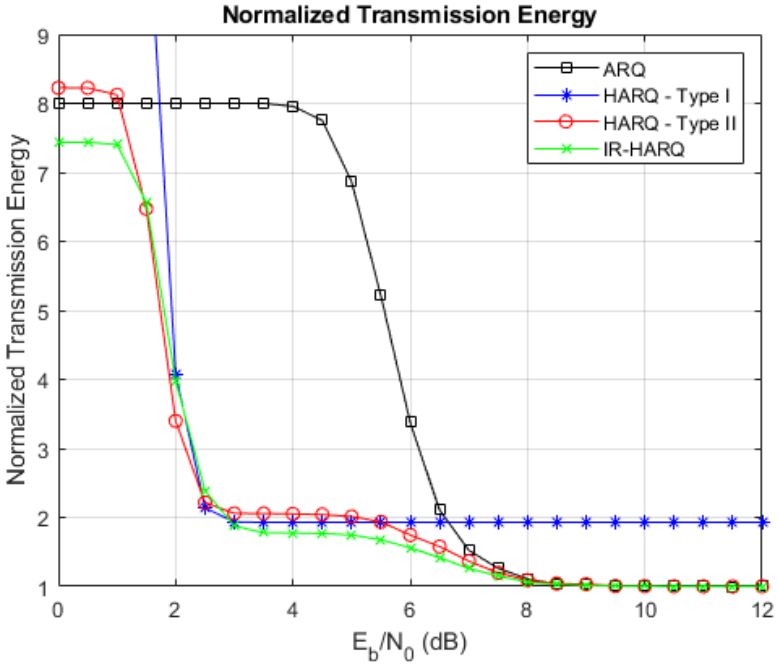

Figure 5.35: Normalized Energy (Eight Scenario)

In Figure 5.35 the starting value for HARQ - Type I is around fifteen times the reference value. The comprehensive analysis of the data presented in Figures 5.32 to 5.35 reveals that the trends and conclusions drawn from experiments involving larger packet sizes also hold when examining scenarios with smaller packet sizes. These findings provide crucial insights into the performance of the IR-HARQ scheme and its behaviour across varying packet sizes and SNR conditions.

Specifically, it is evident that IR-HARQ demonstrates superior efficiency across a wider span of the spectrum, regardless of whether we are dealing with larger or smaller packet sizes.

Scenario Conclusions

Upon closer examination and comparison of the obtained results with both our previous findings and conclusions, a clear conclusion emerges: the advantages of utilizing IR-HARQ persist and hold true even when dealing with smaller packet sizes. This discovery is particularly significant as it aligns with the reality of many IoT devices, which often transmit data in compact packets due to their constrained resources and energy-efficient operation.

5.9 Ninth Scenario - Gilbert-Elliott Channel

In this specific scenario, we are introducing a transmission channel that is characterized and simulated using a Gilbert-Elliott model. Our primary objective in this context is to conduct a comprehensive assessment by comparing and contrasting various performance metrics across different channel models, each defined by distinct values of Time Between Bursts (abbreviated as Tg - Tgood) and Average Burst Duration (referred to as Tb - Tbad).

Across all comparisons, the average burst duration is Tb = 5 bits. Firstly, we compare the performance of ARQ schemes in an AWGN channel and multiple Gilbert-Elliott channels.

To verify the correct implementation of the GE channel model, a similar validation to the one shown in Figure 4.1 was executed, with the results shown in the following figure.

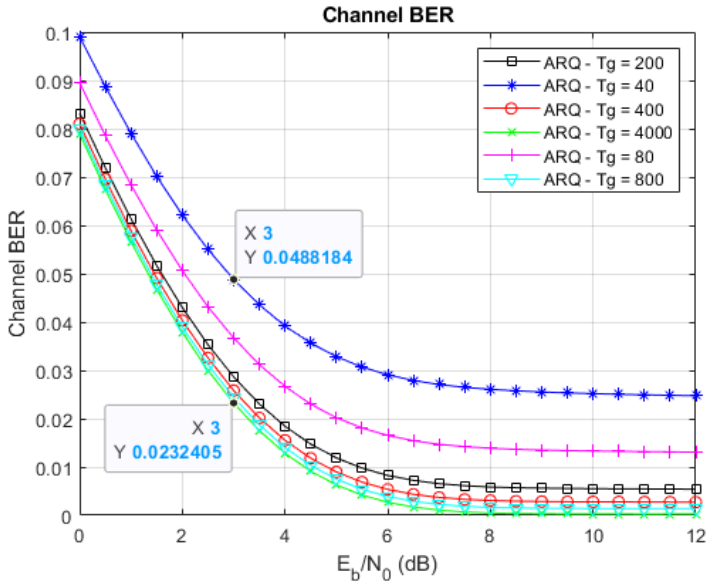

Figure 5.36: Example of the Channel BER plot of the GE channel when well calibrated.

As shown in Figure 5.36, the channel model is functioning correctly, approaching the behaviour of an AWGN channel as Tg rises. On the other hand, when Tg lowers, the Channel BER increases significantly.

5.9.1 ARQ comparison

Firstly, we compare the performance of ARQ schemes in an AWGN channel and multiple Gilbert-Elliott channels.

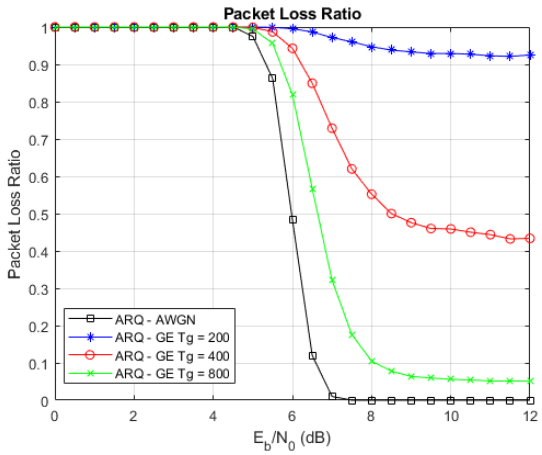

(a) Packet Loss Ratio

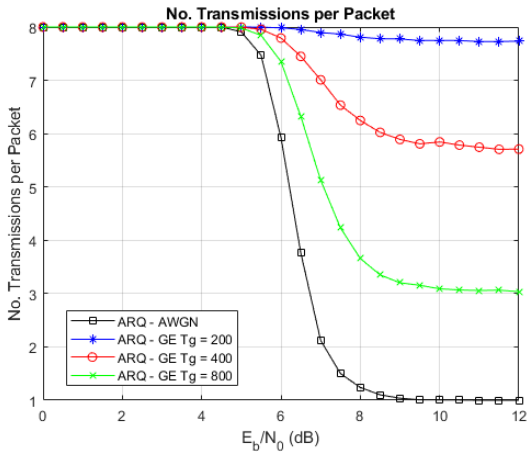

(b) Average Transmissions per Packet

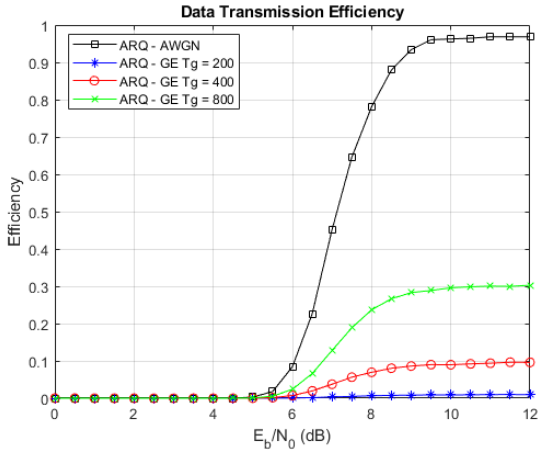

(c) Data Transmission Efficiency

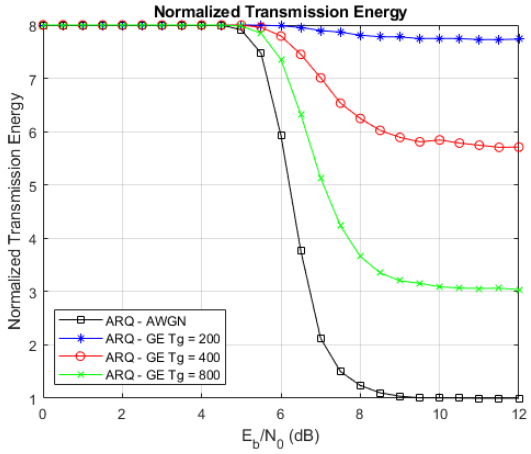

(d) Normalized Energy

Figure 5.37: Diagram Representations of all Metrics (Ninth Scenario - ARQ)

The graphical representations provided in Figure 5.37 illustrate a noteworthy trend that emerges as the time interval between bursts, denoted as Tg, is reduced.

Observing these figures shows that as Tg diminishes, the metrics performance consistently deteriorates. This decline in performance is uniform across all the metrics under consideration. The growing impact of burst errors on the transmitted packet can explain the observed occurrences. These burst errors result in a situation where the number of errors within the packet surpasses the error correction capabilities of the Reed-Solomon algorithm.

5.9.2 All Schemes Comparison with Gilbert-Elliott Tg = 800

In our next step to evaluate all schemes under a Gilbert-Elliott channel, we analyse the schemes' performance when Tg is set to 800.

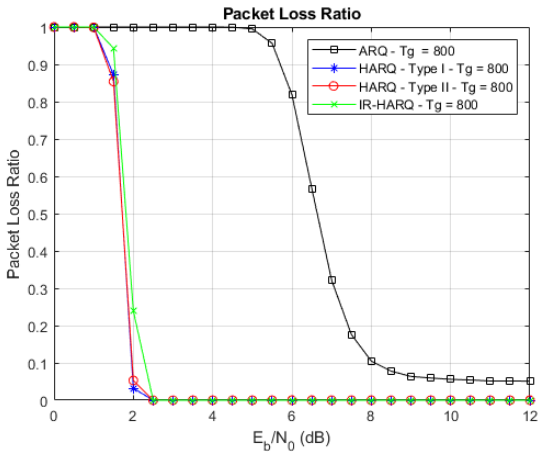

(a) Packet Loss Ratio

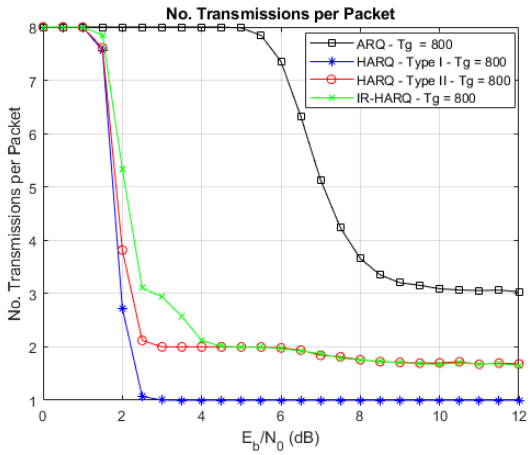

(b) Average Transmissions per Packet

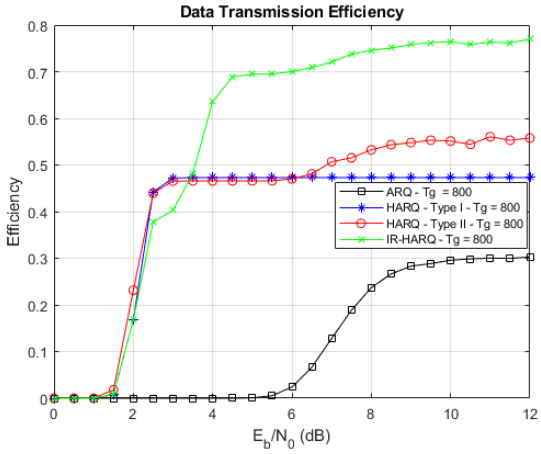

(c) Data Transmission Efficiency

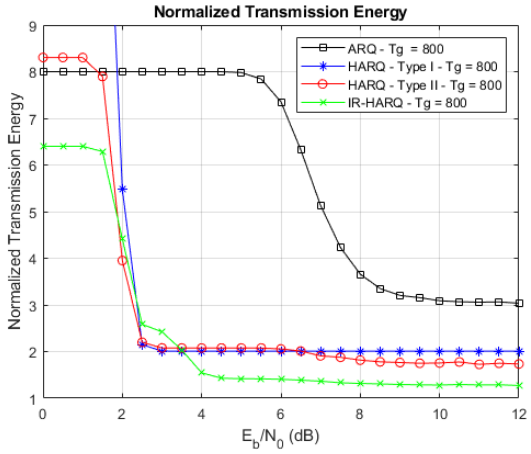

(d) Normalized Energy

Figure 5.38: Diagram Representations of all Metrics (Ninth Scenario - Tg = 800)

As can be seen in Figure 5.38 even in a Gilbert-Elliott channel, in this case with a Tg equal to 800, IR-HARQ proves to retain the same advantages as shown in AWGN channels. It is the most efficient with the highest efficiency in a large range of the SNR scale and somewhat comparable performance in the rest.

Furthermore, it is crucial to emphasize the noteworthy energy efficiency advantages exhibited by the IR-HARQ scheme, especially when confronted with scenarios characterized by high SNR. In an analysis against its counterparts, HARQ Type I and Type II, IR-HARQ emerges as a more energy-efficient solution. Notably, as SNR levels rise to higher magnitudes, IR-HARQ's energy consumption is nearly halved when compared to the energy requirements of HARQ Types I and II under similar conditions.

As mentioned in earlier chapters, it's important to note that the IR-HARQ scheme, while generally robust, does exhibit some trade-offs in certain performance aspects. Specifically, there is a minor decline in its performance regarding the average number of transmissions and packet loss, but this occurs only within a narrow range of SNR. In Figure 5.38d the starting value for

HARQ - Type I is sixteen times the reference.

5.9.3 All Schemes Comparison with Gilbert-Elliott Tg = 400

Following our previous analysts, the next step in our evaluation is to determine if the same truths hold for worse channel conditions. For this effect, we will evaluate the schemes when Tg is equal to 400, meaning that the bursts are twice as probable.

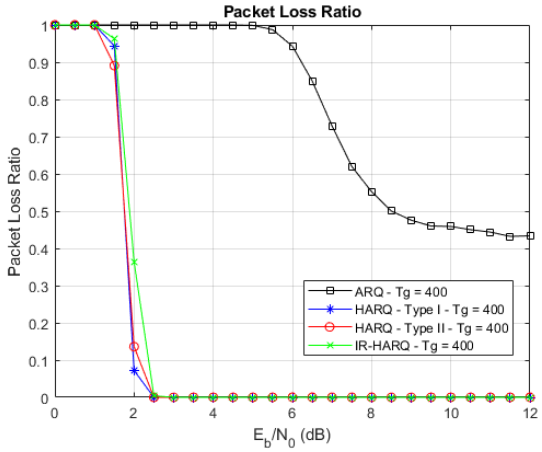

(a) Packet Loss Ratio

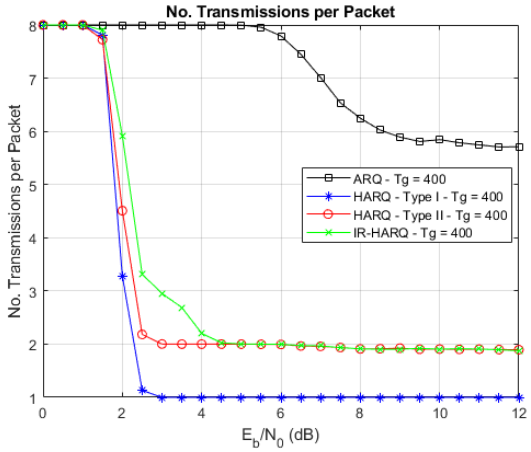

(b) Average Transmissions per Packet

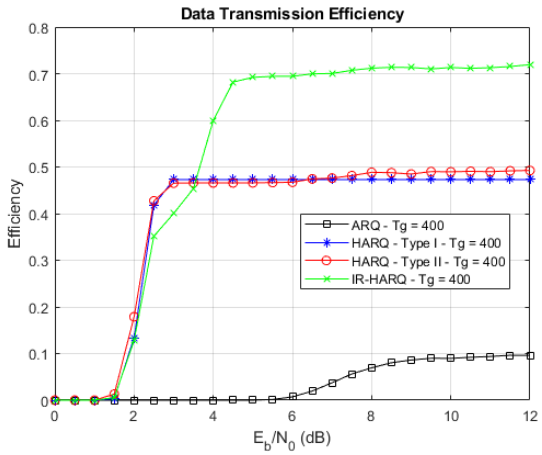

(c) Data Transmission Efficiency

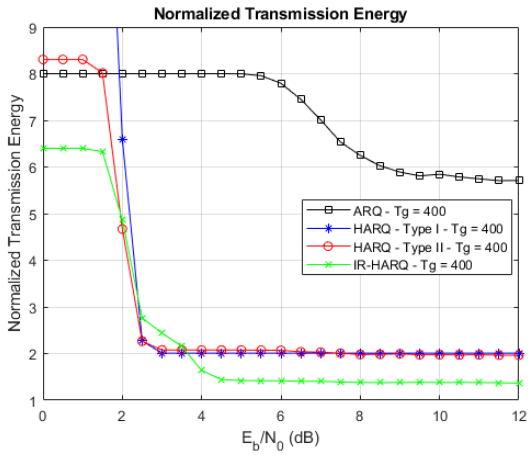

(d) Normalized Energy

Figure 5.39: Diagram Representations of all Metrics (Ninth Scenario - Tg = 400)

In Figure 5.39d the starting value for HARQ - Type I is sixteen times the reference. As depicted in Figure 5.39, the same trends observed for Tg = 800 remain largely consistent when Tg is reduced to 400. IR-HARQ's performance retains its robustness, but as anticipated, there is a slight decrease in efficiency in the face of a more challenging channel. This drop in efficiency is expected in the context of a channel with faster fluctuations between "good" and "bad" states.

5.9.4 All Schemes Comparison with Gilbert-Elliott Tg = 200

Finally, we will use the worst of our defined channel conditions to evaluate all the schemes.

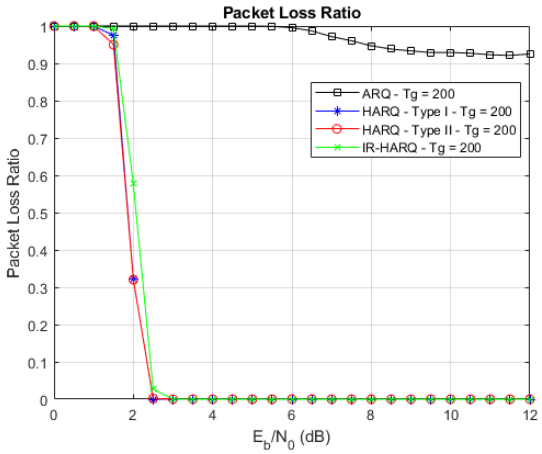

(a) Packet Loss Ratio

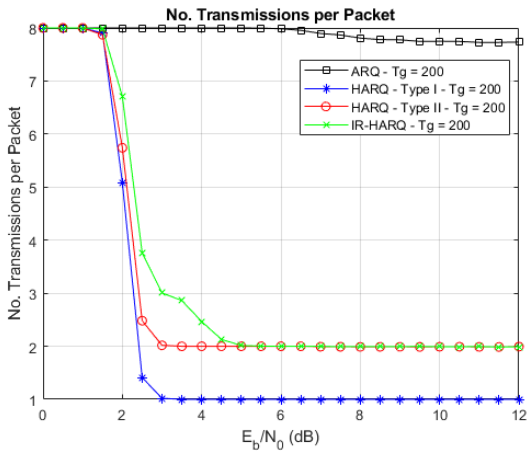

(b) Average Transmissions per Packet

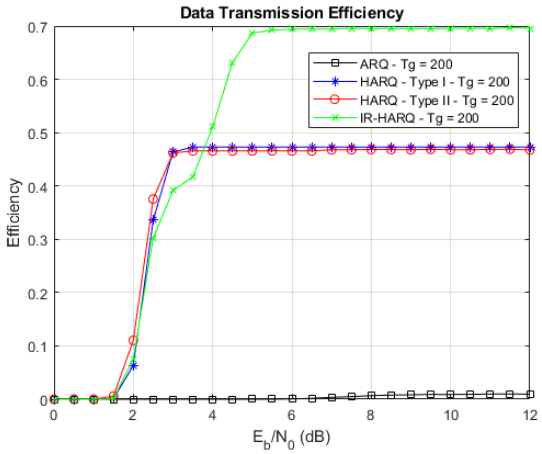

(c) Data Transmission Efficiency

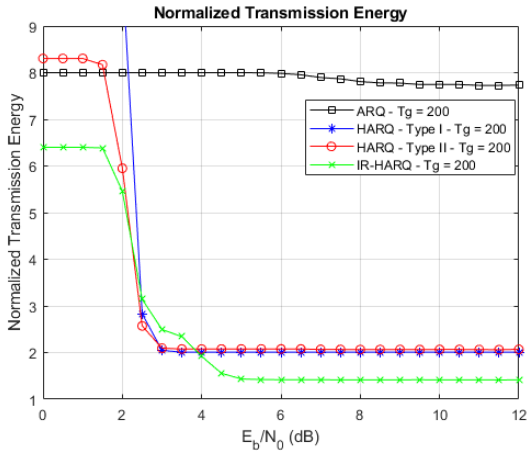

(d) Normalized Energy

Figure 5.40: Diagram Representations of all Metrics (Ninth Scenario - Tg = 200)

In Figure 5.40d the starting value for HARQ - Type I is sixteen times the reference.

As depicted in Figure 5.40, the same trends observed for Tg = 800 and Tg = 400 remain largely consistent when Tg is reduced to 200. IR-HARQ's performance retains its robustness, but as anticipated, there is a slight decrease in efficiency in the face of a more challenging channel. Once more, this slight efficiency decline is observed, but is expected when facing a more turbulent channel environment.

5.9.5 IR-HARQ and HARQ - Type I comparison on Gilbert-Elliot Channels

To further analyse and compare IR-HARQ with other schemes, we will first compare the IR and Type I schemes under all Gilbert-Elliott channels.

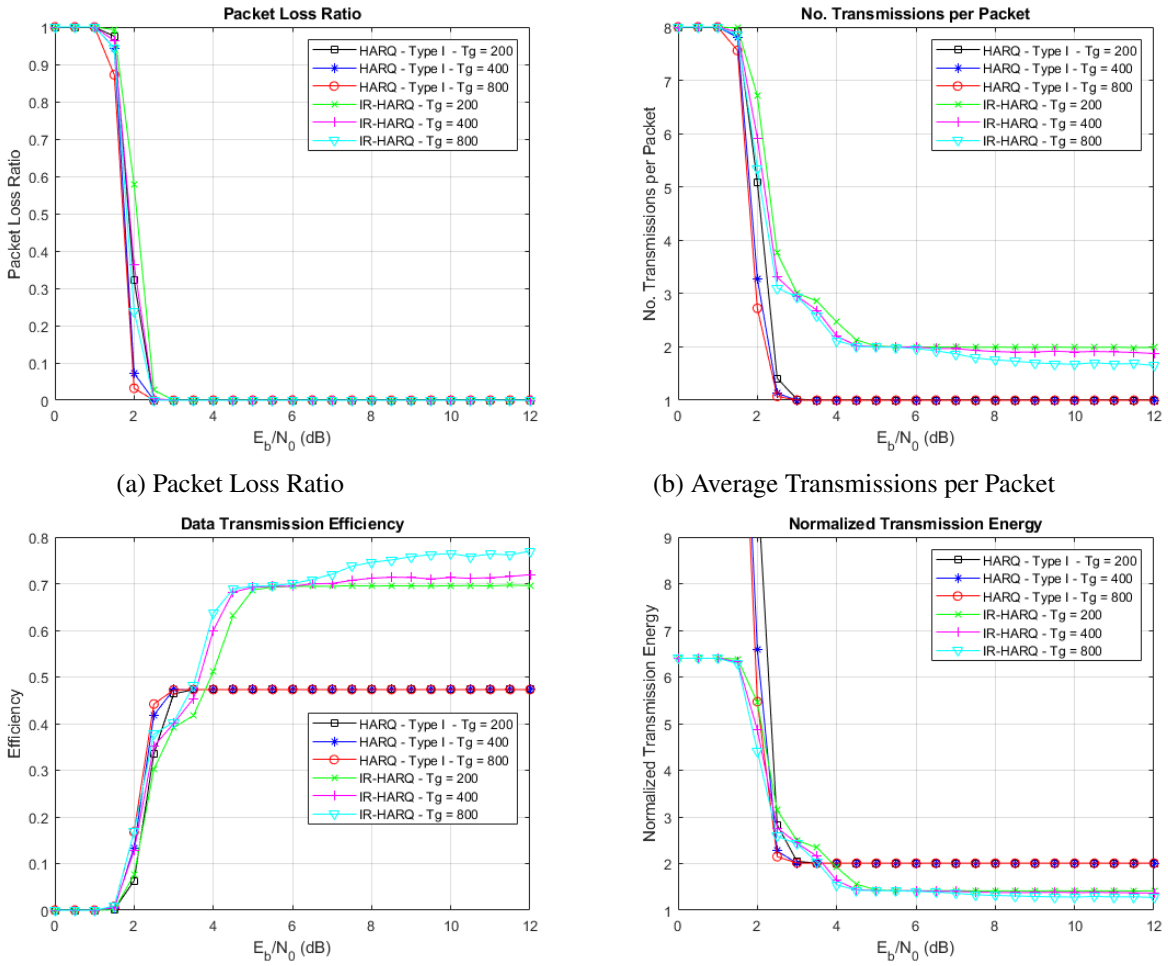

(a) Packet Loss Ratio

(b) Average Transmissions per Packet

(c) Data Transmission Efficiency

(d) Normalized Energy

Figure 5.41: Diagram Representations of all Metrics (Ninth Scenario - IR and Type I)

In Figure 5.41d the starting value for HARQ - Type I is sixteen times the reference. As shown in Figure 5.41, all Incremental schemes are more efficient than their HARQ - Type I counterparts and improve as Tg increases.

Meanwhile, HARQ - Type I shows no improvement as Tg increases, proving less efficient and energy efficient. Its only advantage over the incremental scheme is its smaller number of transmissions, as it can successfully transmit on the first try. However, this one transmission consumes more energy than the two needed for IR-HARQ, as seen in Figure 5.41d.

5.9.6 IR-HARQ and HARQ - Type II comparison on Gilbert-Elliot Channels

Finally, we will compare the IR-HARQ and HARQ - Type II schemes across all Gilbert-Elliott channels.

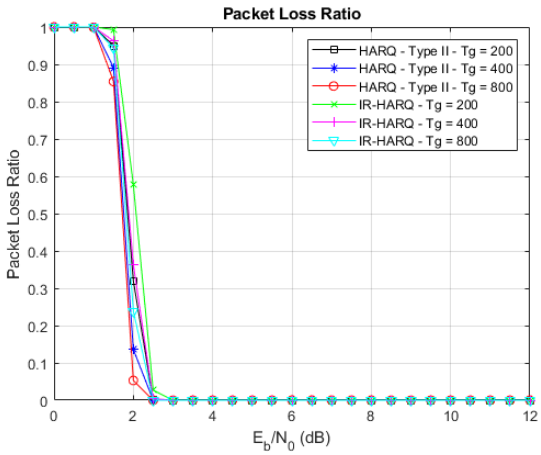

(a) Packet Loss Ratio

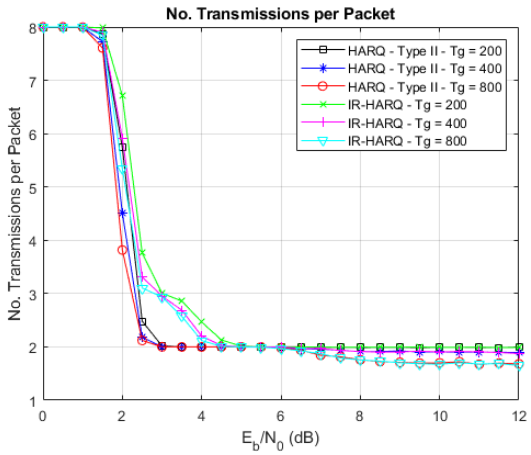

(b) Average Transmissions per Packet

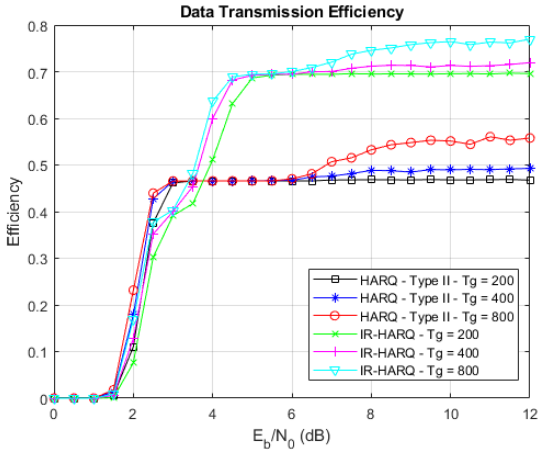

(c) Data Transmission Efficiency

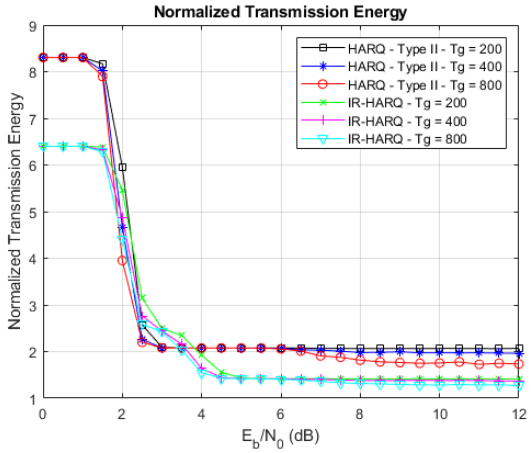

(d) Normalized Energy

Figure 5.42: Diagram Representations of all Metrics (Ninth Scenario - IR and Type II)

As depicted in Figure 5.42, the Incremental schemes consistently outperform HARQ - Type II in terms of efficiency in identical conditions. Although both scheme types exhibit a modest efficiency boost, IR-HARQ consistently maintains a substantial lead. The Incremental schemes also showcase superior energy efficiency, highlighting their effectiveness.

5.9.7 Scenario Conclusions

While the Gilbert-Elliott or burst error model proves to be a more challenging channel for all schemes, IR-HARQ exhibits relatively consistent performance across different channel conditions, starkly contrasting to ARQ, which displays significant variations. Furthermore, when compared to HARQ - Type I and II, IR-HARQ maintains a considerable advantage. The analyses made in this section show that both HARQ - Type I and IR-HARQ have their benefits and drawbacks. In the context of wireless sensor networks, it's worth noting that IR-HARQ proves to be a more efficient communication protocol. However, it exhibits some disadvantages when considering delays compared to Type I protocols, which show a smaller delay and fewer retransmissions per packet. In

these networks, the emphasis is often placed on conserving energy rather than prioritizing low delay times. Therefore, IR-HARQ has more benefits even in channels modelled by a Gilbert-Elliott model.

Chapter 6

Conclusions and Future Work

This chapter presents a summary of the work developed, along with reinstating the major contributions and limitations of the simulator. It will also touch on some points for possible future work.

6.1 Work Outline

The main objective of this dissertation was to enhance the understanding of Incremental Redundancy Hybrid Automatic Repeat Request (IR-HARQ) by exploring additional metrics not covered in the existing literature. This was achieved by creating a specialized simulator capable of evaluating and analysing various factors and scenarios related to IR-HARQ and ARQ schemes in general.

The research began by highlighting the importance of studying the efficiency of incremental schemes, driven by the growing demand for energy-efficient and reliable data transmission methods, especially in relation to the Internet of Things (IoT). As the need for dependable communication and reduced retransmissions becomes crucial, investigating more robust schemes like IR-HARQ gains significance.

To lay the groundwork for the study, the dissertation extensively reviewed the state-of-the-art in the field, delving into the available literature on ARQ and Hybrid ARQ schemes. Each of these schemes, along with some error correction codes, was introduced and examined to establish a comprehensive understanding of the current landscape.

Moreover, the dissertation acknowledged the unique challenges posed by sensor networks and the emerging issue of high energy consumption. To address these concerns, Incremental Redundancy HARQ was presented as a potential solution with its advantages and suitability for the identified problems.

The subsequent focus was on developing a sophisticated simulator capable of simulating diverse scenarios by adjusting parameters and variables. This simulator served as a valuable tool to conduct experiments, gather data, and gain insights into the performance of IR-HARQ under various conditions.

In the final phase of the research, all the accumulated data were thoroughly analysed and compared across different scenarios. The primary goal was to validate the effectiveness of the proposed IR-HARQ solution. Additionally, this analysis provided critical feedback to refine and optimize both the simulator and the functioning of the IR-HARQ scheme itself. This iterative process aimed to improve the overall performance and applicability of IR-HARQ in real-world sensor networks.

In conclusion, this dissertation contributed to the IR-HARQ field by comparing not often-studied metrics, designing an adaptable and configurable simulator, and conducting in-depth analyses. By enhancing the understanding of IR-HARQ's capabilities and limitations, this research shed light on possible more complex solutions and their benefits, especially in the context of sensor networks. The findings also served as a foundation for future research and potential advancements in this critical area of study.

6.2 Future Work

Moving forward, several avenues for future work are identified to enhance and extend the capabilities of the developed simulator.

To broaden the scope of the simulator's analysis, incorporating additional modulations and FEC codes is essential. Including a wider range of modulation techniques will allow for a more comprehensive examination of different transmission schemes. Moreover, integrating various FEC codes will enable a comparison of their performance under different scenarios.

To mimic real-world scenarios more accurately, introducing different types of transmission channels, such as noisy channels or multipath channels, will be valuable. Additionally, integrating fading effects, like Rayleigh or Rician fading, will provide insights into the behaviour of IR-HARQ under more challenging and dynamic communication conditions.

Currently, the simulator has been developed and tested with a specific number of nodes in the system. However, in practical applications, sensor networks can vary significantly in size. Expanding the simulator to handle varying numbers of nodes will allow for a better understanding of the scalability and performance implications of IR-HARQ in different network sizes.

A promising avenue for further advancement is to incorporate intelligence into the simulator. By implementing adaptive algorithms, the system can dynamically detect and analyse channel conditions [32]. Based on this analysis, the simulator can optimize the selection of modulation, FEC codes, and retransmission strategies to maximize the likelihood of successful data transmission with the least number of attempts. This intelligent adaptation will make the simulator more realistic and relevant to modern communication systems.

By pursuing these directions, the simulator can be further enhanced and serve as a powerful tool for research.

References

[1] Giuseppe Durisi, Tobias Koch, and Petar Popovski. Toward massive, ultrareliable, and low-latency wireless communication with short packets. *Proceedings of the IEEE*, 104:1–16, 08 2016. doi:10.1109/JPROC.2016.2537298.

[2] *Cellular Networks for Massive IoT: Enabling Low Power Wide Area Applications*. Ericsson, Stockholm, Sweden, 2016.

[3] Soojin Cho, Billie Spencer, Hongki Jo, Jian Li, and Robin Kim. Bridge monitoring using wireless smart sensors. *SPIE Newsroom*, 01 2011. doi:10.1117/2.1201212.004043.

[4] Mario Rodriguez. Channel simulation in wireless communication, with python code, Dec 2022. URL: https://mario-rodriguez.medium.com/channel-simulation-in-wireless-communication-with-python-code-cd4f65805192.

[5] E. N. Gilbert. Capacity of a burst-noise channel. *The Bell System Technical Journal*, 39(5):1253–1265, 1960. doi:10.1002/j.1538-7305.1960.tb03959.x.

[6] E. O. Elliott. Estimates of error rates for codes on burst-noise channels. *The Bell System Technical Journal*, 42(5):1977–1997, 1963. doi:10.1002/j.1538-7305.1963.tb00955.x.

[7] Michael Short, Imran Sheikh, Syed Aley, and Imran Rizvi. Bandwidth-efficient burst error tolerance in tdma-based can networks. In *ETFA2011*, pages 1–8, 2011. doi:10.1109/ETFA.2011.6058999.

[8] B. Vucetic and J. Yuan. *Turbo Codes: Principles and Applications*. The Springer International Series in Engineering and Computer Science. Springer US, 2012. URL: https://books.google.pt/books?id=QgrrBwAAQBAJ, doi:10.1007/978-1-4615-4469-2.

[9] Martin Riley and Iain Richardson. reed-solomon codes, 1996. (accessed Jul. 26 2023). URL: https://www.cs.cmu.edu/~guyb/realworld/reedsolomon/reed_solomon_codes.html.

[10] Irving S. Reed and Gustave Solomon. Polynomial codes over certain finite fields. *Journal of The Society for Industrial and Applied Mathematics*, 8:300–304, 1960.

[11] Stephen B Wicker and Vijay K Bhargava. *Reed-Solomon codes and their applications*. John Wiley & Sons, Nashville, TN, September 1999.

[12] C. Berrou, A. Glavieux, and P. Thitimajshima. Near shannon limit error-correcting coding and decoding: Turbo-codes. 1. In *Proceedings of ICC '93 - IEEE International Conference on Communications*, volume 2, pages 1064–1070 vol.2, 1993. doi:10.1109/ICC.1993.397441.

[13] M.C. Reed and S.S. Pietrobon. Turbo-code termination schemes and a novel alternative for short frames. In *Proceedings of PIMRC '96 - 7th International Symposium on Personal, Indoor, and Mobile Communications*, volume 2, pages 354–358 vol.2, Oct 1996. doi:10.1109/PIMRC.1996.567415.

[14] Gregory Mitchell. Investigation of hamming, reed-solomon, and turbo forward error correcting codes. page 24, 07 2009.

[15] Erdal Arikan. Channel polarization: A method for constructing capacity-achieving codes for symmetric binary-input memoryless channels. *IEEE Trans. Inf. Theor.*, 55(7):3051–3073, jul 2009. URL: https://doi.org/10.1109/TIT.2009.2021379, doi:10.1109/TIT.2009.2021379.

[16] Seo Jeong, Jung Bae, and Myung Sunwoo. Fast multibit decision polar decoder for successive-cancellation list decoding. *Journal of Signal Processing Systems*, 93, 01 2021. doi:10.1007/s11265-020-01570-x.

[17] Christopher Graham Blake. *Energy Consumption of Error Control Coding Circuits*. PhD thesis, University of Toronto, Toronto, Ontario, Canada, 2017.

[18] Darija Čarapić, Mirjana Maksimovic, and Miodrag Forcan. Performance analysis of ldpc and polar codes for message transmissions over different channel models. In *8th International Conference on Electronics, Telecommunications, Computing, Automatics and Nuclear Engineering - IcETRAN 2021*, 09 2021.

[19] Lorenzo Vangelista and Marco Centenaro. Performance evaluation of harq schemes for the internet of things. *Computers*, 7, 12 2018. doi:10.3390/computers7040048.

[20] Anoosheh Heidarzadeh, Jean-Francois Chamberland, Richard D. Wesel, and Parimal Parag. A systematic approach to incremental redundancy with application to erasure channels. *IEEE Transactions on Communications*, 67(4):2620–2631, 2019. doi:10.1109/TCOMM.2018.2889254.

[21] Peihong Yuan, Fabian Steiner, Tobias Prinz, and Georg Böcherer. Flexible ir-harq scheme for polar-coded modulation. In *2018 IEEE Wireless Communications and Networking Conference Workshops (WCNCW)*, pages 49–54, 2018. doi:10.1109/WCNCW.2018.8369005.

[22] Endrit Dosti, Mohammad Shehab, Hirley Alves, and Matti Latva-Aho. Ultra reliable communication via optimum power allocation for harq retransmission schemes. *IEEE Access*, 8:89768–89781, 2020. doi:10.1109/ACCESS.2020.2994277.

[23] Mohammad Sadegh Mohammadi, Iain B. Collings, and Qi Zhang. Simple hybrid arq schemes based on systematic polar codes for iot applications. *IEEE Communications Letters*, 21:975–978, 5 2017. doi:10.1109/LCOMM.2017.2662012.

[24] Bang Wang. Coverage problems in sensor networks: A survey. *ACM Comput. Surv.*, 43(4), oct 2011. URL: https://doi.org/10.1145/1978802.1978811, doi:10.1145/1978802.1978811.

[25] Nilufa Yeasmin. k-coverage problems and solutions in wireless sensor networks: A survey. *International Journal of Computer Applications*, 100:1–6, 2014. URL: https://api.semanticscholar.org/CorpusID:3437160.

[26] Archana Bharathidasan and Vijay Anand Sai Ponduru. Sensor networks: An overview. In *IEEE INFOCOM*, volume 4. Citeseer, 2002.

[27] Youngbok Cho, Minkang Kim, and Sunghee Woo. Energy efficient iot based on wireless sensor networks. In *2018 20th International Conference on Advanced Communication Technology (ICACT)*, pages 294–299, 2018. doi:10.23919/ICACT.2018.8323730.

[28] Kagiso More, Christian Wolkersdorfer, Ning Kang, and Adel Elmaghraby. Automated measurement systems in mine water management and mine workings – a review of potential methods. *Water Resources and Industry*, 24:100136, 08 2020. doi:10.1016/j.wri.2020.100136.

[29] Elisa Bertino. Data security and privacy in the iot. In *EDBT*, volume 2016, pages 1–3, 2016. doi:10.5441/002/edbt.2016.02.

[30] Matlab. (accessed Jul. 26 2023). URL: https://www.mathworks.com/products/matlab.html.

[31] TheNeuralBit. Theneuralbit/ece5565-harq. (accessed Jul. 26 2023). URL: https://github.com/TheNeuralBit/ece5565-harq.

[32] Apostolos Avranas, Marios Kountouris, and Philippe Ciblat. The influence of csi in ultra-reliable low-latency communications with ir-harq. In *2019 IEEE Global Communications Conference (GLOBECOM)*, pages 1–6, 2019. doi:10.1109/GLOBECOM38437.2019.9013553.